Biochimica et Biophysica Acta 1848 (2015) 1927–1943

Contents lists available at ScienceDirect

Biochimica et Biophysica Acta

journal homepage: www.elsevier.com/locate/bbamem

Review

Folding of β-barrel membrane proteins in lipid bilayers — Unassisted and assisted folding and insertion☆

Jörg H. Kleinschmidt *

Abteilung Biophysik, Institut für Biologie, FB 10, Universität Kassel and Center for Interdisciplinary Nanostructure Science and Technology (CINSaT), Heinrich-Plett-Str. 40, D-34132 Kassel, Germany

ARTICLE INFO

Article history:
Received 22 March 2015
Received in revised form 6 May 2015
Accepted 7 May 2015
Available online 14 May 2015

Keywords:
β-barrel membrane protein
Membrane protein folding
Kinetics
Outer membrane
Periplasmic chaperone
BAM complex
OmpA

ABSTRACT

In cells, β-barrel membrane proteins are transported in unfolded form to an outer membrane into which they fold and insert. Model systems have been established to investigate the mechanisms of insertion and folding of these versatile proteins into detergent micelles, lipid bilayers and even synthetic amphipathic polymers. In these experiments, insertion into lipid membranes is initiated from unfolded forms that do not display residual β-sheet secondary structure. These studies therefore have allowed the investigation of membrane protein folding and insertion in great detail. Folding of β-barrel membrane proteins into lipid bilayers has been monitored from unfolded forms by dilution of chaotropic denaturants that keep the protein unfolded as well as from unfolded forms present in complexes with molecular chaperones from cells. This review is aimed to provide an overview of the principles and mechanisms observed for the folding of β-barrel transmembrane proteins into lipid bilayers, the importance of lipid–protein interactions and the function of molecular chaperones and folding assistants. This article is part of a Special Issue entitled: Lipid–protein interactions.

Contents

Abbreviations: C, cysteine; CAC, critical association concentration; CD, circular dichroism; $diC_{10:0}$PC, 1,2-dicapryl-*sn*-glycero-3-phosphocholine; $diC_{12:0}$PC, 1,2-dilauroyl-*sn*-glycero-3-phosphocholine; $diC_{12:0}$PE, 1,2-dilauroyl-*sn*-glycero-3-phosphoethanolamine; $diC_{12:0}$PG, 1,2-lauroyl-*sn*-glycero-3-phosphoglycerol; $diC_{14:0}$PC, 1,2-dimyristoyl-*sn*-glycero-3-phosphocholine; $diC_{18:1}$PC, 1,2-dioleoyl-*sn*-glycero-3-phosphocholine; $diC_{18:1}$PE, 1,2-dioleoyl-*sn*-glycero-3-phosphoethanolamine; $diC_{18:1}$PG, 1,2-dioleoyl-*sn*-glycero-3-phosphoglycerol; F, phenylalanine; FomA, major outer membrane protein A from *Fusobacterium nucleatum*; hVDAC1, voltage-dependent anion-selective channel, human isoform 1; KTSE, Kinetics of Tertiary Structure Formation by Electrophoresis; LPS, lipopolysaccharide; LUVs, large unilamellar vesicles; OM, outer membrane; OmpA, OmpC, OmpF, OmpG, OmpT, OmpW, and OmpX, outer membrane proteins A, C, F, G, T, W, and X from *Escherichia coli* (see also Table 1); OMP, outer membrane protein; PAGE, polyacrylamide gel electrophoresis; PagP, lipid A palmitoyltransferase from *E. coli*; SDS, sodium dodecylsulfate; Skp, seventeen kilodalton protein; SurA, survival factor A; SUVs, small unilamellar vesicles; TM, transmembrane; TMP, transmembrane protein; TMD, transmembrane domain; VDAC, voltage-dependent anion-selective channel; W, tryptophan; wt, wild-type; Y, tyrosine.

☆ This article is part of a Special Issue entitled: Lipid–protein interactions.

* Tel.: +49 561 804 4041; fax: +49 561 804 934041.
E-mail address: jhk@uni-kassel.de.

http://dx.doi.org/10.1016/j.bbamem.2015.05.004
0005-2736/

1. Introduction

Biological membranes are essential structuring components of all living cells. The core elements of membranes are lipid bilayers and integral and peripheral proteins. While a lipid bilayer constitutes the hydrophobic barrier of a membrane and prevents the arbitrary exchange of solutes, transmembrane proteins (TMPs)[a] allow the regulated exchange of solutes across the lipid bilayer or they transduce signals from one side of the membrane to the other. Many membrane proteins perform enzymatic reactions, which take place at the membrane–water interface. Specific lipid–protein interactions are important for the stable integration and activity of integral and peripheral membrane proteins (see, *e.g.* [1–3]). The unique structure of the lipid bilayer requires specific surface properties of integral and peripheral proteins that are necessary for their function. Protein surfaces exposed to the fatty core of the membrane are typically hydrophobic, while protein surfaces exposed to the aqueous space usually are composed of polar amino acid residues. These properties of membrane proteins have raised strong interest to examine the physical principles, how integral proteins fold and insert into membranes (see, *e.g.*, [4–7]). TMPs can be subdivided into two classes according to their transmembrane (TM) structure, namely α-helical TMPs and TMPs with β-sheet secondary structure in the lipid bilayer. While TMPs with a single TM helix are common [8], all TMPs with β-sheet secondary structure known to date form closed β-barrels with at least 8 antiparallel TM β-strands. In these β-barrels, all β-strands are connected to their next neighbors through hydrogen bonds between the amide-protons and the carbonyl groups of the polypeptide backbone. The β-barrel structure is closed through hydrogen bonds formed between the amino-terminal and the carboxy-terminal membrane-spanning β-strands. The strands of β-barrel TMPs are connected by short periplasmic β-turns and by long loops facing the polysaccharide region and the space outside the cell or cell organelle. The geometry of the β-strands and the necessity to form hydrogen bonds between polar amide and carbonyl groups of the polypeptide chain within the hydrophobic core of the membrane exclude that individual β-strands can exist in a lipid bilayer. In the TM region of a β-barrel, polar and apolar residues alternate with one another: the β-strands are amphipathic. The hydrophobic residues face the apolar lipid phase, while polar residues face the barrel lumen, across which nutrients in aqueous solution are transported. Therefore in comparison to α-helical TMPs, the average hydrophobicity of TM β-barrels is low. With the exception of the capsule transporter Wza [9], all currently known outer membrane proteins (OMPs) from bacteria form β-barrel TM structure. β-barrel TMPs are also found in the outer membranes (OMs) of mitochondria and chloroplasts. Some representative examples are shown in Fig. 1. β-barrel TMPs are characterized by the number of antiparallel β-strands and by the shear number, which is a measure for the inclination angle of the β-strands against the barrel axis [10]. The OMPs of known crystal structure from bacteria form TM β-barrels with even numbers of β-strands ranging from 8, like in the TM domain (TMD) of outer membrane protein A (OmpA) from *Escherichia coli*, to 26 in the lipopolysaccharide (LPS) channel LptD. The voltage-dependent anion-selective channel, human isoform 1 (hVDAC1) from mitochondria forms a β-barrel with 19 TM strands. OMPs exist as monomers (for example OmpA, BtuB), dimers (OmPlA) or trimers (ScrY, LamB). OMPs can be grouped into at least 10 different categories regarding their function [7,11]. They may serve as structural proteins (for example OmpA), as toxin binding proteins (OmpX), as passive unspecific diffusion porines (OmpF, OmpC), as specific porines (LamB, ScrY, FadL, Tsx), as active transporters (BtuB, FhuA), as proteases (OmpT), lipases (OmPlA), or acyltransferases (PagP), as adhesion proteins (NspA, OpcA), as insertion machines (BamA), as pilus assembly plattforms (PapC, FimD), as export channels (TolC), *etc.* Some OMPs of known crystal structure of their β-barrel domains are listed in Table 1, together with their molecular weights, pI, number of TM β-strands in the β-barrel domain, number of amino acid residues, oligomeric state and function. In this review, we provide an overview of the observations and biophysical principles of folding and membrane insertion of β-barrel membrane proteins into lipid bilayers of defined composition.

2. Denaturation and refolding of β-barrel transmembrane proteins

OmpA is the first TMP for which successful refolding was shown. In 1978, Schweizer et al. [12] demonstrated that more than 90% of heat-denatured OmpA (Omp II [13]) regained its native structure in the presence of LPS and Triton-X-100. Later, Dornmair et al. [14] established that OmpA can refold in micelles of octylglucoside in the absence of LPS after dilution of the denaturants, sodium dodecyl sulfate (SDS) or urea. Further experiments demonstrated that urea-denatured OmpA can be folded both in lipids and in a wide range of detergents, provided that the concentration is above the CAC [15]. OmpA folds even from certain fragments in micelles of octylglucoside [16,17], an observation first made *in vivo* for separately expressed fragments [18]. Later, very large β-barrel TMPs like the 22-stranded iron transporter FepA, which contains an additional domain in the barrel lumen, have been refolded successfully from their denatured forms in chaotropic denaturants into detergent micelles upon denaturant dilution [19]. The list of successfully refolded β-barrels also includes the 19-stranded human VDAC from the OM of mitochondria [20–23]. Interestingly, circular dichroism (CD) spectra indicated that human VDAC, isoform 1, develops slightly different secondary structure in LDAO detergent micelles than in lipid bilayers of various phospholipids [20]. In LDAO/*di*$C_{12:0}$PC mixtures, the β-sheet content decreased from ~37% in pure *di*$C_{12:0}$PC bilayers to ~32% in pure LDAO micelles, whereas the content of α-helical secondary structure increased from ~11% to ~16%. A change of 5% in secondary structure corresponds to about 14 residues out of 282 residues in VDAC. This is not a very large fraction, but could be enough to form an additional transmembrane β-strand at the expense of some of the α-helical structure obtained for the detergent solubilized form. Expression of β-barrel TMPs in form of cytosolic inclusion bodies and subsequent refolding has in fact become a major strategy for the isolation of many β-barrel TMPs (for a recent review, see *e.g.*, Ref. [24]). A

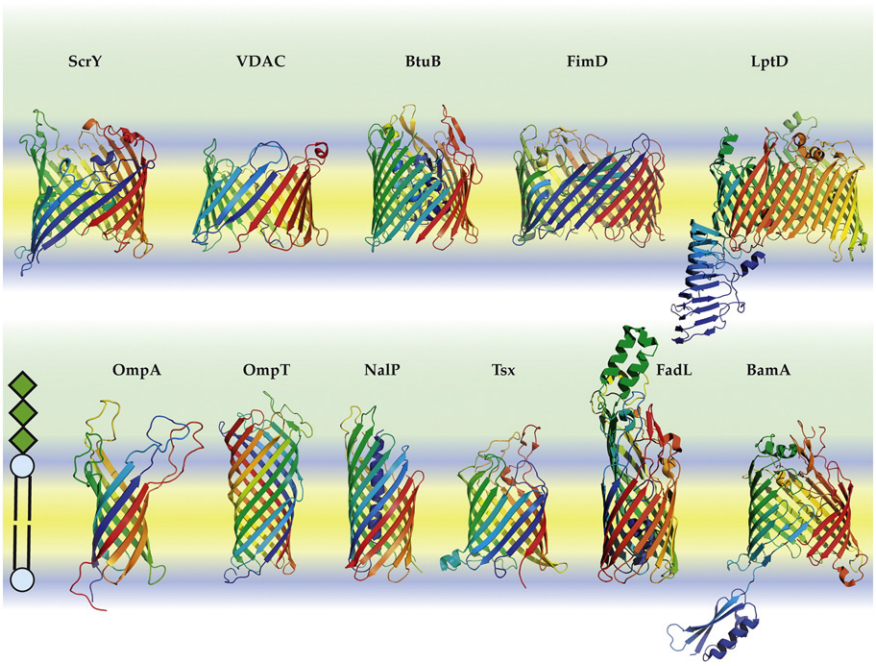

Fig. 1. Representative structures of β-barrel TMDs of outer proteins are shown. TM β-barrels from Gram-negative bacteria have an even number of antiparallel TM strands, which is 8 for OmpA (shown here is the NMR structure from Ref. [157], for the crystal structure see Refs. [158,159]), 10 for OmpT [160], 12 for NalP [161] or Tsx (Ye and van den Berg, 2004), 14 for FadL [162], 16 for BamA (shown here is the structure of BamA from *E. coli* [163] with one out of the five periplasmic POTRA domains), 18 for ScrY [164], 22 for BtuB [165], 24 for FimD [166] and 26 for LptD [167]. The voltage-dependent anion selective channel (hVDAC) from human mitochondria forms a 19-stranded TM β-barrel, in which the *amino*- and *carboxy*-terminal strands are parallel (shown here is the NMR structure [168,169]). As a structural protein [170] and a small ion channel [31] OmpA is linked to the peptidoglycan *via* its periplasmic domain (~145 residues, not shown). OmpT is a protease, NalP is an autotransporter, Tsx is a nucleoside specific diffusion porin, FadL is a long chain fatty acid transporter, BamA a main component of the barrel assembly machinery complex, ScrY is a sucrose specific porin. BtuB is an active transporter for vitamin B_{12} uptake and FimD is the type 1 pilus assembly plattform. LptD is mediating LPS transport into the outer leaflet of the OM of Gram-negative bacteria. Protein structures were generated with MacPyMol [171] (see also http://www.pymol.org).

commonly observed feature of most β-barrels is a shift in the electrophoretic mobility between the folded and unfolded forms when the samples are not heat-denatured before electrophoresis. For OmpA, the unfolded form migrates at an apparent molecular mass of ~35 kDa, while the folded form migrates at ~30 kDa. For larger β-barrels, the shift in the electrophoretic migration can be even greater, in case of iron receptor FhuA from 78 kDa for the unfolded to 54 kDa for the folded form [7]. For smaller OMPs, like for the β-barrel domain of OmpA (residues 1–171), the shift can be reversed, *i.e.* the folded form migrates slower than the unfolded form. After complex formation with SDS, small 8-stranded β-barrel domains have a lower electrophoretic mobility when folded. This is caused by a lower charge/mass ratio, because less SDS is bound. Apparently, the larger β-barrels with greater volume and hydrophobic surface bind much more SDS in their folded state, increasing the charge–mass ratio and electrophoretic mobility relative to the unfolded state, thus leading to a faster migration. Different SDS-loading capacities and correspondingly positive or negative shifts in the electrophoretic mobility, have also been reported for α-helical membrane proteins [25].

The change in the electrophoretic mobility is an indicator for the formation of native structure as demonstrated in numerous investigations on the structure and function of β-barrel TMPs. For example, for wild-type (wt)-OmpA, all structural and functional experiments have shown identity between the 30 kDa form and structurally intact and fully functional OmpA. These previous studies included analyses of the OmpA structure by Raman [26], Fourier transform infrared [27], and CD spectroscopy [14,15,28,29], biochemical digestion experiments [28,30], and functional assays such as phage inactivation [12], and single channel conductivity measurements [31]. Similar observations were made for larger β-barrel TMPs, for example the major outer membrane protein A from *Fusobacterium nucleatum* (FomA) [32].

3. Folding of β-barrel membrane proteins into lipid bilayers from chaotropic denaturants

3.1. Unfolding and solubilization of β-barrel TMPs for folding studies

To describe the mechanisms of membrane protein folding, defined model systems are required to explore intermediates and transition states for folding and membrane insertion. Since TMPs are composed of hydrophobic residues in their TMDs, their unfolding and solubilization is often a major challenge. CD spectroscopy indicates that the β-pleated sheet secondary structure of β-barrel TMPs is completely destroyed in concentrated solutions of chaotropic denaturants like urea or guanidinium chloride, but molecular dynamics studies suggest that some tertiary contacts remain [33], even at high denaturant concentrations. Similar tertiary contacts might also exist during translocation of unfolded OMPs in cells, like in the periplasm of Gram-negative bacteria after the unfolded OMPs emerge from the SecYEG translocon of the cytoplasmic membrane. Folding of denaturant-unfolded OMPs can be studied by dilution of the denaturant in the presence of detergent micelles (see, *e.g.*, [14,15,34–36]), lipid bilayers (see *e.g.*, [20,28,30,32,36–43]) or even synthetic amphipathic polymers (see, *e.g.*, [44–46], see also Ref. [47] for a recent review). In folding studies, the artificial denaturant urea can be replaced successfully by an *in vitro* translation system for OMPs [48].

3.2. Conditions for OMP folding into lipid bilayers and oriented folding

To examine the biophysical principles of β-barrel membrane protein folding, model systems ideally should mimic a membrane environment, but should contain only as few components as necessary. The successful refolding of urea-unfolded OMPs like OmpA into detergent led to the

Table 1
Examples of outer membrane proteins of known high-resolution structure.

OMPs with single-chain β-barrels

OMP	Organism	MW (kDa)	pI[a]	Residues	Residues in β-barrel domain	β-strands in barrel domain	Oligomeric state	Function	PDB entry	Refs.
OmpA	*E. coli*	35.2	5.6	325	171	8	Monomer	Structural	1QJP, 1BXW	[158,159]
OmpA[b]	*E. coli*	35.2	5.6	325	171	8	Monomer	Structural	1G90	[157]
OmpW	*E. coli*	20.9	5.6	191	191	8	Monomer	Structural	2F1T, 2F1V	[176]
OmpX	*E. coli*	16.4	5.3	148	148	8	Monomer	Toxin binding	1QJ8	[177]
OmpX[b]	*E. coli*	16.4	5.3	148	148	8	Monomer	Toxin binding	1Q9F	[178]
NspA	*N. meningitidis*	16.6	9.5	153	153	8	Monomer	Cell adhesion	1P4T	[179]
PagP	*E. coli*	19.5	5.9	166	166	8	Monomer	Palmitoyl transferase	1THQ	[180]
PagP[b]	*E. coli*	19.5	5.9	166	166	8	Monomer	Palmitoyl transferase	1MM4, 1MM5	[181]
OmpT	*E. coli*	33.5	5.4	297	297	10	Monomer	Protease	1I78	[160]
OpcA	*N. meningitidis*	28.1	9.5	254	254	10	Monomer	Adhesion protein	1K24	[182]
Tsx	*E. coli*	31.4	4.9	272	272	12	Monomer	Nucleoside uptake	1TLW, 1TLY	[183]
NalP[c]	*N. meningitidis*	28.9	6.7	298	265	12	Monomer	Autotransporter	1UYN	[161]
OmPlA[d]	*E. coli*	30.8	5.1	269	269	12	Dimer	Phospholipase	1QD6	[184]
OmpG	*E. coli*	32.8	4.4	280		14	Monomer	Porin	2IWW, 2F1C	[185,186]
FadL	*E. coli*	45.9	4.9	421	378	14	Monomer	Fatty acid transporter	1T16, 1T1L	[162]
BamA	*E. coli*	88.4	4.9	790	390	16	Monomer	β-barrel insertion	4N75	[163,187]
BamA	*N. gonorrhoeae*	85.7	8.8	771	372	16	Monomer	β-barrel insertion	4K3B	[61]
Omp32	*C. acidovorans*	34.8	8.8	332	332	16	Trimer	Porin	1E54	[188]
Porin	*R. capsulatus*	31.5	4.0	301	301	16	Trimer	Porin	2POR	[189,190]
Porin	*R. blastica*	30.6	3.8	290	290	16	Trimer	Porin	1PRN	[191]
OmpF	*E. coli*	37.1	4.6	340	340	16	Trimer	Porin	2OMF	[192]
PhoE	*E. coli*	36.8	4.8	330	330	16	Trimer	Porin	1PHO	[192]
OmpK36	*K. pneumoniae*	37.6	4.4	342	342	16	Trimer	Porin	1OSM	[193]
LamB	*E. coli*	47.4	4.7	420	420	18	Trimer	Maltose specific porin	1MAL, 1AF6	[194,195]
Maltoporin	*S. typhimurium*	48.0	4.7	427	427	18	Trimer	Maltose specific porin	2MPR	[196]
ScrY	*S. typhimurium*	53.2	5.0	483	415	18	Trimer	Sucrose porin	1A0S, 1A0T	[164]
VDAC	*H. sapiens*	30.6	8.6	282	257	19	Monomer	Voltage-dependent channel	2K4T, 2JK4	[168,169]
FhuA	*E. coli*	78.7	5.1	714	587	22	Monomer	Ferrichrome iron transporter	2FCP, 1BY3	[197,198]
FepA	*E. coli*	79.8	5.2	724	574	22	Monomer	Ferrienterobactin transporter	1FEP	[199]
FecA	*E. coli*	81.7	5.4	741	521	22	Monomer	Iron (III) dicitrate transporter	1KMO, 1PNZ	[200,201]
BtuB	*E. coli*	66.3	5.1	594	459	22	Monomer	Vitamin B_{12} transporter	1NQE, 1UJW	[202,203]
FpvA	*P. aeruginosa*	86.5	5.1	772	538	22	Monomer	Ferripyoverdine transporter	1XKH	[204]
FimD	*E. coli*	91.4	6.0	833	526	24	Monomer	Type 1 pilus assemb. plattf.	3OHN, 3RFZ	[166]
PapC	*E. coli*	92.3	6.4	843	505	24	Dimer	Type P pilus assemb. plattf.	2VQI	[205]
LptD	*S. flexneri*	87.1	4.9	759	560	26	Monomer	LPS assembly protein	4Q35	[167]

OMPs with multi-chain β-barrels

Organism	OMP	MW (kDa)	pI	Residues	Residues in β-barrel domain	β-strands in barrel domain	Chains in the β-barrel	Function	PDB entry	Refs.
TolC	*E. coli*	51.5	5.2	471	285 (95 × 3)	12 (4 × 3)	Trimer	Export channel	1EK9	[206]
MspA	*M. smegmatis*	17.6	4.4	168	432 (32 × 8)	16 (2 × 8)	Octamer	Porin	1UUN	[207]
α-Hemolysin	*S. aureus*	33.2	7.9	293	378 (54 × 7)	14 (2 × 7)	Heptamer	Toxin	7AHL	[208]

[a] Calculated by Protparam/SWISS-PROT.
[b] NMR structure.
[c] Translocator domain.
[d] OmpLA dimerizes transiently during its function and is otherwise present as a monomer.

exploration of insertion and folding of β-barrel TMPs into pure lipid bilayers [28,37]. OmpA was the first β-barrel TMP, for which insertion and folding into lipid bilayers upon urea-dilution was shown [28]. Folding was demonstrated for bilayers of small unilamellar vesicles (SUVs) of dimyristoylphosphatidyl choline (*di*$C_{14:0}$PC) in the liquid-crystalline (fluid) phase. Below the phase-transition temperature, OmpA adsorbed to the bilayer surface and formed β-sheet secondary structure, but did not insert into the bilayer. Its apparent molecular mass remained at 35 kDa and surface adsorbed OmpA was also completely degradable by trypsin. OmpA aggregates and precipitates upon urea-dilution in the absence of lipid bilayers or detergent. This pathway must be suppressed by selecting favorable conditions for folding, like protein and lipid concentrations. The third requirement for insertion and folding of OmpA was the use of highly curved SUVs of *di*$C_{14:0}$PC [28]. The early examinations of lipid membrane insertion and folding of OmpA all relied on the use of phospholipids with myristoyl (C_{14}) or longer chains [27–30,37,38,49]. In theses cases, the preparation of SUVs was a prerequisite for successful folding and bilayer insertion, which has been attributed to the presence of defects in SUVs [28,30]. Defects in SUVs were previously [50] and also recently [51] described to facilitate the reconstitution of detergent-solubilized TMPs. An increased number of defects in the bilayer structure, present at the phase transition temperature from the gel to the fluid phase, and the coexistence of phase boundaries were recently shown to promote TMP insertion [52]. Lipid vesicles are usually not permeable to solutes, but defects in lipid organization could serve as nucleation sites for membrane protein insertion. Insertion and folding of the β-barrel include the formation of the barrel pore and the translocation of the polar outer loops of OMPs across the bilayer. This requires an additional, even larger disturbance of the bilayer structure than caused by pre-existing defects in pure lipid vesicles. Therefore and for other reasons discussed below, the activation energy required for bilayer insertion is lower for thinner lipid bilayers that are more flexible [53] and for membranes that are under curvature stress [54]. Curved and more flexible bilayers likely also facilitate conformational changes in membrane adsorbed, partially folded OMPs. The protein/lipid interface and stoichiometry, protein–lipid selectivity, and the orientation of inserted β-barrel OMPs have been examined by electron spin resonance spectroscopy and by FTIR spectroscopy [55–57].

Even smaller β-barrels, like the 8-stranded transmembrane domain of OmpA, are surrounded by at least 11 diacylphospholipids, indicating that insertion of a β-barrel requires the displacement of many lipids, which is faster in thinner, more flexible membranes. The hydrophobic thickness of many β-barrel membrane proteins is ~20–25 Å [39]. For ButB, it varies around the β-barrel between 18 and 23 Å [58]. This corresponds to the hydrocarbon region of thin bilayers, like those of $di C_{12:0}$PC, which is 19.5 ± 0.1 Å [39,59]. Interestingly, electron microscopy [60] has revealed notches in lipid bilayers containing BamA, which is an essential TMP for the insertion of OMPs into the OM of bacteria. These disturbances of the lipid bilayer by BamA could be functionally relevant and are likely related to the structure of BamA [61], which shows that the hydrophobic thickness of the transmembrane domain is asymmetric as first described for BtuB [58]. This asymmetry could cause large distortions of the lipid bilayer in proximity to BamA, as suggested by molecular dynamics simulations [61], which likely facilitate insertion and folding of unfolded OMPs.

Interestingly, insertion and folding of β-barrel membrane proteins into lipid bilayers is oriented, as could be demonstrated for the barrel domains of OmpA [28] and later also BamA [62].

3.3. Monitoring the kinetics of insertion and folding of β-barrel TMPs by electrophoresis

The most direct method to examine the kinetics of insertion and folding of β-barrel membrane proteins exploits the different electrophoretic mobilities of folded and unfolded forms. In a kinetic assay, SDS is added to small volumes of the reaction mixture that are taken out at defined times after initiation of folding. In these samples, SDS binds quickly to folded and unfolded OmpA and prevents further folding of OmpA. At room temperature, SDS does not denature OmpA that has folded. Therefore, at the end of the kinetic experiment, the fraction of folded OmpA in each sample can be determined by cold SDS-polyacrylamide gel electrophoresis (PAGE) (*i.e.* without heat-denaturing the samples) and subsequent densitometry of the bands of folded and unfolded OmpA [30]. This method monitors the formation of tertiary structure in OmpA as a function of time (Kinetics of Tertiary Structure Formation by Electrophoresis, KTSE) [63]. The method has been used successfully in later studies for several other β-barrel membrane proteins like FomA [32], the lipid A palmitoyl transferase from *E. coli* (PagP) [40,64], OmpX [43], OmpT [42] and others. The method has the advantage that the effect of folding facilitators like periplasmic chaperones or proteins of the barrel assembly machinery (BAM) complex can be examined without much interference in the analysis, because all proteins are usually separated in SDS-PAGE and folded and unfolded forms of the β-barrel TMP can be easily distinguished [62,65,66]. As folding intermediates are usually not stable enough to resist unfolding by SDS at room temperature, the KTSE analysis reports the last phase of folding, the formation of the native β-barrel.

3.4. Parallel folding processes

Early examinations of the kinetics of OmpA folding into lipid bilayers of 1,2-dioleoyl-*sn*-glycero-3-phosphocholine ($di C_{18:1}$PC) at neutral or basic pH using the KTSE analysis, suggested a single phase for the last folding step monitored by electrophoresis, because a single exponential function could be fitted to the experimental time courses [30]. For bilayers of $di C_{18:1}$PC, a single phase of folding was observed even in the presence of a chaperone, the seventeen kDa protein (Skp, see Section 4 below), provided the experiment was performed at a pH ≥ 7 and analyzed by KTSE [66]. In contrast, a double exponential time course was necessary to describe the time course of folding of another OMP, namely FomA at pH 10, when analyzed using the KTSE method. This indicated the presence of two parallel folding processes of FomA [32]. These parallel processes likely arise from two different folding intermediates of the OMP, IM_1 and IM_2 (in the case of FomA because the experiment was performed in a titration region, see Fig. 2C). IM_1 and IM_2 are both converted to the folded β-barrel OMP, but at different rates:

$$IM_1 - k_f \rightarrow (F \cdot L)_f \quad \text{(fast)}$$

$$IM_2 - k_f \rightarrow (F \cdot L)_s \quad \text{(slow)}$$

Here $(F{\cdot}L)_f$ and $(F{\cdot}L)_s$ both describe a folded β-barrel OMP in a membrane, but as a result of a faster (index *f*) or slower (index *s*) folding process. The total concentration of the folded β-barrel OMP is given by the

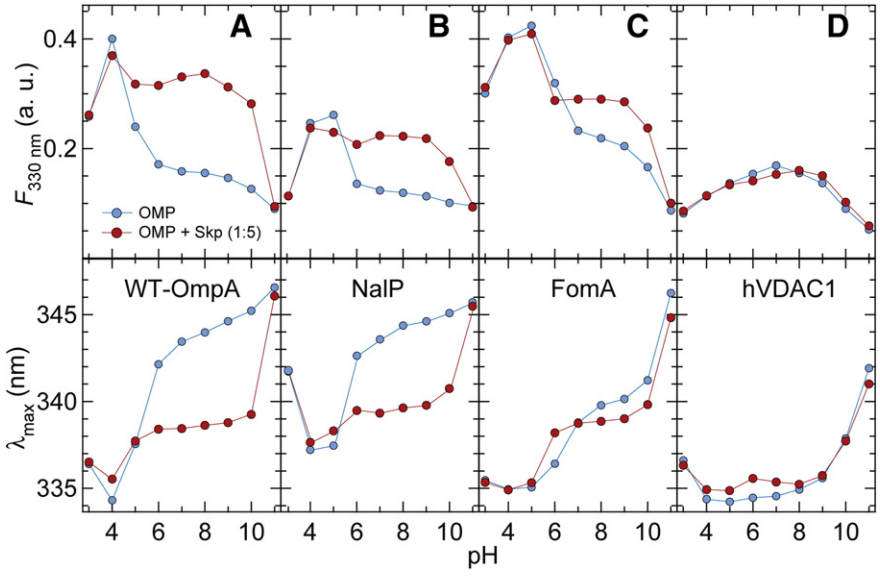

Fig. 2. Different conformational states of OMPs coexist in aqueous solution in the absence of lipids. Shown is the pH-dependence of the fluorescence signals of several OMPs in aqueous solution in the absence and in the presence of the periplasmic chaperone Skp for 0.43 μM OmpA (A), 0.47 μM NalP (B), 0.20 μM FomA (C) and 0.65 μM hVDAC1 (D). Fluorescence spectra of these OMPs were recorded for the aqueous forms in the absence (○) and in the presence (●) of a 5-fold molar excess of Skp as a function of pH between pH 3 and pH 11. The wavelength of the fluorescence emission maximum (λ_{max}) and the fluorescence intensities at 330 nm obtained upon excitation at 295 nm are plotted as a function of pH. At this wavelength, the fluorescence of Skp is negligible as it does not contain any W residues.
Adapted from Ref. [73].

sum of the concentrations of folded β-barrel OMP formed in the fast and in the slow process: $[F{\cdot}L](t) = [(F{\cdot}L)_f](t) + [(F{\cdot}L)_s](t)$. To date, all evidence for kinetic experiments on the folding of OMPs suggest that the last folding step, the formation of the folded barrel, is rate limiting and that intermediates are formed on a much faster time-scale than the folded barrel. In the electrophoretic analysis, the sum $[(IM)_1](t) + [(IM)_2](t) + [F{\cdot}L](t)$ would then be approximately equal to the total concentration of the β-barrel protein in the system. At high lipid concentration, the rate of folding is given by the sum of two independent pseudo-first order folding processes with the rate constants k_f for the fast and k_s for the slow folding process:

$$\frac{d[F\cdot L]}{dt} = \frac{d[(F\cdot L)_f]}{dt} + \frac{d[(F\cdot L)_s]}{dt} = -\frac{d[IM_1]}{dt} - \frac{d[IM_2]}{dt} = k_f[IM_1] + k_s[IM_2]. \quad (1)$$

Integration and substitution of the concentrations by mole fractions leads to

$$X_{F\cdot L} = 1 - \left[X_{IM_{1,0}} \cdot \exp(-k_f \cdot t) + X_{IM_{2,0}} \cdot \exp(-k_s \cdot t)\right] \quad (2)$$

where $X_{IM1,0}$ and $X_{IM2,0}$ are the extrapolated mole fractions of the intermediate forms IM_1 and IM_2 for $t \to 0$ min. Since at $t \to 0$ min, the fraction of the folded β-barrel OMP $X_{F\cdot L,0} \to 0$, it follows that the sum $X_{IM1,0} + X_{IM2,0} = 1$ and the equation can be further simplified to

$$X_{F\cdot L}(t) = 1 - \left[A_f \exp\{-k_f t\} + (1 - A_f)\exp\{-k_s t\}\right] \quad (3)$$

where A_f is the contribution of the faster process in the last folding stage to the overall folding yield of the β-barrel OMP. This model also includes the (alternative) possibility that not all of the β-barrel TMP folds, *i.e.*, $k_s = 0$. Eq. (3) can then be transformed to

$$X_{FP}(t) = A_f \cdot \left[1 - \exp\{-k_f \cdot t\}\right]. \quad (4)$$

In this case, A_f corresponds to the folding yield. Eqs. (3) and (4) have been successfully used to analyze experimental time courses of folding obtained by electrophoresis. This includes the analysis of the last stage of the folding of β-barrels like OmpA and FomA under a variety of different conditions [32]. It also includes the analysis of folding of OmpA performed in the presence of molecular chaperones [66] or BamA, the main component of the BAM folding machine [62]. The relative contribution of the fast folding process can be modulated. For FomA, A_f increases with temperature. Thinner and therefore more flexible bilayers [67] also favor the contribution of the faster process of insertion and folding of FomA into lipid bilayers at a lipid/FomA ratio of ~1000/1 [7,32].

Similar observations of the role of membrane flexibility in parallel folding pathways were also made for the 8-stranded β-barrel PagP [68]. PagP folded into an 800-fold excess of 1,2-dilauroyl-*sn*-glycero-3-phosphocholine (diC$_{12:0}$PC) within 5 min to its catalytically active form. At a residual concentration of 7 M urea, a single exponential time course was sufficient to describe the folding kinetics obtained by CD spectroscopy for secondary and tertiary structure formation. In contrast, parallel folding processes of PagP were observed at diC$_{12:0}$PC/PagP ratios of 1600, 3200 and above [41,68]. Incorporation of 1,2-dilauryl-*sn*-glycero-3-phosphoethanolamine (diC$_{12:0}$PE) into diC$_{12:0}$PC resulted in an increase of the relative contribution of the slower folding process. It is known that a higher content of diC$_{12:0}$PE in mixed diC$_{12:0}$PC/diC$_{12:0}$PE membranes decreases the flexibility of the bilayer [69,70]. Increased PagP folding rates in more flexible bilayers are consistent with the reports on OmpA and FomA [32,39,53].

3.5. Consecutive folding steps

Folding steps that precede the last stage of membrane insertion and folding of β-barrel TMPs have to be analyzed using techniques other than KTSE, like fluorescence, CD or infrared spectroscopy, as the KTSE assay rarely reports on events preceding the formation of native structure. In general, the sensitivity of each technique toward the investigated folding step must be checked carefully. The usefulness of any methodology may be limited to certain steps of membrane protein folding. For example, fluorescence or CD spectroscopy may also report on protein aggregation in addition to folding and before these techniques can be fully exploited, the extent of aggregation of TMPs will have to be estimated. This can elegantly be done for example by analytical ultracentrifugation [71]. Tan et al. [71] have reported that high urea concentrations maintain all investigated OMPs, namely OmpA, OmpW, OmpX, PagP, OmpT, OmpLA, FadL, and Omp85, soluble. Even after dilution to 1 M urea OmpA and OmpX remained monomeric [71]. The study also revealed that a residual presence of urea could be useful for the optimization of folding experiments as previously described for folding of OmpG into detergent. For folding of OmpG into micelles of octylglucoside, a residual concentration of 3 M urea led to higher folding yields in comparison to 1 M urea or below [72]. This experiment also showed that the formation of folded OmpG dimers is suppressed at 3 M urea. The 8-stranded β-barrel PagP, required the presence of at least 5 M urea for significant folding into lipid bilayers of diC$_{12:0}$PC [40], but did not fold at all when the denaturant urea was diluted to a final concentration of 4 M or less. Optimal folding yields were obtained at 6–7 M urea and even at a residual urea concentration of 8 M, almost half of the PagP folded [40].

3.6. Different aqueous folding intermediates can be distinguished by fluorescence spectroscopy

The observation of two parallel folding processes in the analyses of the KTSE experiments is explained by the coexistence of two intermediate aqueous forms, IM_1 and IM_2. Their presence is evident from fluorescence spectroscopy of the aqueous forms of several OMPs (Fig. 2) [73]. For FomA (pI 8.6), the shift in the wavelength of the fluorescence emission maximum (Fig. 2C) and the fluorescence intensity at 330 nm indicate a titration at pH ~ 10, the pH at which folding of FomA into bilayers of phosphatidylcholine was examined earlier [32]. Similarly other OMPs display titrations in other pH regions. For example, folding of OmpA is characterized by two parallel kinetic processes in KTSE experiments, when folding into bilayers of diC$_{18:1}$PC is performed below pH 7 [66], in the titration region of OmpA (Fig. 2A) [73]. Changes in the fluorescence of aqueous folding intermediates indicate that these intermediates have a different exposure of fluorescent side-chains to the aqueous environment. Since W, which stabilizes the barrel in the membrane [74–76], is most frequently oriented toward the lipid environment in aromatic girdles around a folded β-barrel [77,78], the two titrating aqueous forms will fold *via* different conformation changes. Side chains that form hydrogen bonds with water molecules are dehydrated upon membrane insertion and lipid exposure, as shown for W and tyrosine (Y) residues of the aromatic girdles at the barrel surface [79]. Different hydration of the side-chains, as apparent for the titrating forms of the OMPs shown in Fig. 2, likely affects the insertion and folding kinetics as the activation energy for insertion depends on the initial hydration state of the side-chains.

3.7. Parallel and sequential folding steps and effects of interfacial pH

In KTSE analyses, OmpA displays a single folding process when inserted and folded into bilayers of phosphatidylcholines at basic pH, regardless of the chain length of the phosphatidylcholine used in the experiment [30,32,39,49]. A single kinetic phase was also observed when OmpA was folded into dioleoylphosphatidylcholine from a complex with the chaperone Skp instead of its urea-denatured form [66]. However, parallel folding processes can be observed, when the lipid bilayer also contains negatively charged lipids or mixtures of charged and neutral lipids [66]. Negatively charged lipids in a bilayer lead to an increased proton activity at the surface and therefore to a pH-gradient from the

bulk solution to the membrane–water interface. Even if the bulk pH is basic, the interfacial pH of negatively charged lipid bilayers is likely lower [80–82] and the pH gradient will result in a titration of the membrane bound protein and consequently lead to parallel folding processes of coexisting differently protonated forms of the inserting OMP. For the analysis of sequential events in insertion and folding of OMPs it is important to select conditions at which parallel folding processes are largely suppressed. Fluorescence spectroscopy (Fig. 2) [73] and previous kinetic data [30,66] suggest neutral to basic pH and membranes composed of only phosphatidylcholine are favorable to examine intermediates and intermediate folding phases.

3.8. Folding kinetics in large unilamellar vesicles of short-chain lipids

In 2002, about a decade after folding of OmpA was shown for lipid bilayers of SUVs, it was reported that OmpA can also fold into larger (extruded) vesicles, provided the bilayers are formed of lipids with dodecanoyl (C_{12}) or shorter fatty acyl chains [39]. Folding rates of OMPs into bilayers of short-chains phospholipids increase if the hydrophobic fatty acyl chains are shorter and for OmpA folding, the rates were fastest for 1,2-dicapryl-*sn*-glycero-3-phosphocholine (*di*$C_{10:0}$PC) [39,53]. For bilayers of dilauroyl phosphatidylcholine (*di*C12:0PC), folding of OmpA has been successful with large unilamellar vesicles (LUVs) with a diameter of up to 800 nm [54]. For *di*$C_{12:0}$PC, kinetics of folding, but not folding yields, displayed a strong dependence on the vesicle surface curvature and rates of folding decreased at increased vesicle diameter, when all other conditions were unaltered (Fig. 3). The experiment by Pocanschi et al. [54] (Fig. 3) shows that folding is faster if vesicles of higher overall curvature are prepared from bilayer forming lipids.

The effect of membrane curvature in LUVs and SUVs [54] in addition to membrane thickness [39,53] is important for insertion and folding of β-barrel TMPs. Folding is still observed for thicker bilayers of longer chain phospholipids like 1,2-dimyristoyl-*sn*-glycero-3-phosphocholine (*di*$C_{14:0}$PC) or di$C_{18:1}$PC, provided the vesicles are sufficiently small and under curvature stress. Thinner bilayers are more flexible and membrane flexibility, in the form of out-of-plane bending fluctuations, may lower the activation energy for spontaneous insertion and folding of β-barrel proteins into lipid membranes [39,53]. The membrane–water interface promotes the orientation of polar and apolar side-chains (Fig. 4A) consistent with the formation of β-pleated sheet secondary structure observed for membrane-adsorbed OmpA [27,28]. However, the β-sheets have to form hydrogen bonds with their next neighbors. Flexible and curved membrane surfaces will promote the association of neighboring β-strands as shown in Fig. 4B. This is correlated to the structure of the TM β-strands, which are curved and twisted around the β-barrel surface (Fig. 1). OmpA folded into a range of lipid bilayers composed of phosphatidylcholines and displayed kinetics of second order and a single process of folding and membrane insertion [39]. At high lipid concentration, a simple pseudo first-order rate law could also be fitted to the experimental time course. Interestingly, the rate constants obtained from KTSE assays, which monitors the formation of compact tertiary structure, were very similar to rate constants of OmpA folding kinetics monitored by CD spectroscopy, which monitors the formation of secondary structure. These rate constants were lower, by a factor of 4, than the rate constants monitored by fluorescence spectroscopy, indicating that lipid–protein interactions precede the formation of secondary and tertiary structure [39]. In these experiments with bilayers of short-chain phosphatidylcholine at pH 10, all kinetics were well described by single-exponential (pseudo first order) fit functions, regardless of the method used to monitor folding. This observation was also made when folding experiments were performed with small sonicated vesicles of the long-chain phospholipid *di*$C_{18:1}$PC at 40 °C [30,39] although the rate constants were slower than those obtained for LUVs of *di*$C_{12:0}$PC at 30 °C [39]. Secondary and tertiary structure formation of another OMP, PagP were also characterized by very similar rate constants [40]. In PagP, a Cotton effect between residues Y_{26} and W_{66} gives rise to a maximum in the CD spectrum around 232 nm. This band provides a very sensitive assay for the formation of native PagP. CD spectroscopy could therefore also be used to monitor tertiary structure formation and secondary structure formation in parallel [40].

3.9. Folding and insertion of OmpA in bilayers of dioleoylphosphatidylcholine (SUVs) are synchronized

In fluorescence experiments, multiple kinetic phases indicated the presence of folding intermediates of OmpA in bilayers of *di*$C_{18:1}$PC (SUVs) [30]. Folding of OmpA into lipid membranes of *di*$C_{18:1}$PC (SUVs) is slower than into membranes composed of lipids with shorter acyl chains [39], which facilitates the examination of folding intermediates in particular at lower temperatures. W-fluorescence quenching in combination with kinetic folding experiments [38,49] indicated that

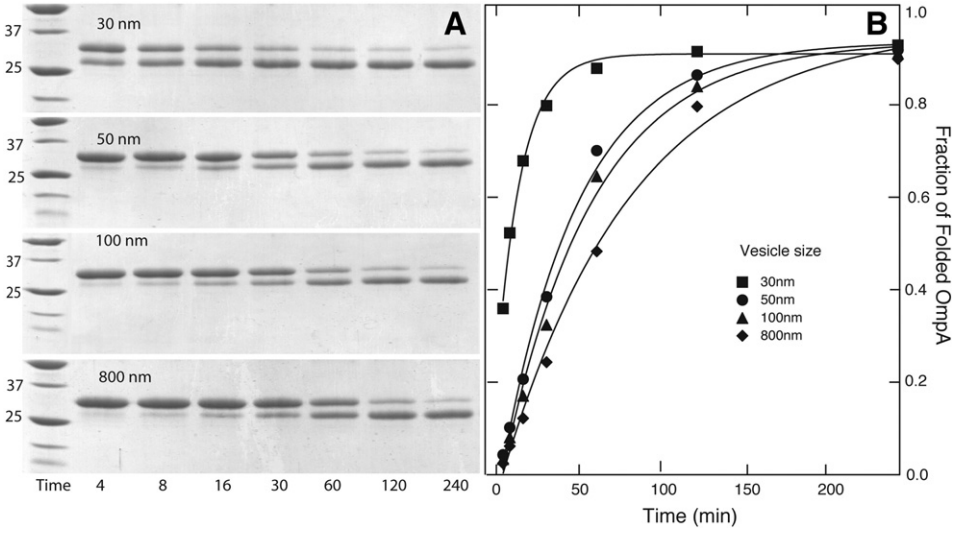

Fig. 3. Folding kinetics of OmpA into *di*$C_{12:0}$PC vesicles of different diameters at 20 °C, prepared either by sonication (vesicles with a 30 nm diameter) or by extrusion (vesicles with diameters from 50 to 800 nm). (A) SDS-PAGE of OmpA (17 μM) at different times of incubation after dilution from urea into 7 mM of *di*$C_{12:0}$PC with vesicle diameters as indicated. Folding is accompanied by a downward gel shift to lower apparent molecular mass. (B) Fraction of folded OmpA with time, determined from gel densitometry.
Adapted from Ref. [54].

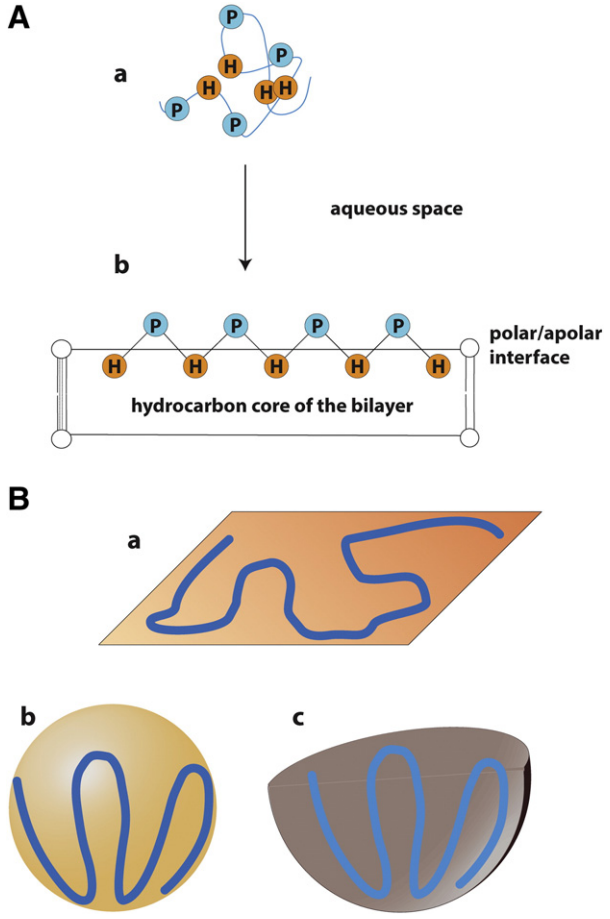

Fig. 4. (A) The polar/apolar interface of the lipid bilayer promotes orientation of hydrophobic and polar residues within the polypeptide chain of β-barrel TMPs. This is important for the formation of the correct hydrogen bonds between neighboring β-strands, because in the final β-barrel structure alternating hydrophobic and polar side-chains are facing the hydrophobic exterior and polar interior of the barrel. In collapsed aqueous forms, hydrophobic residues are likely oriented more toward the interior of these intermediates [125]. (B) Surfaces with either positive (b) or negative (c) curvature promote proximity between neighboring β-strands of a polypeptide chain in comparison to flat surfaces. Therefore, β-barrels like OmpA insert more rapidly into membranes that are thin and flexible (and transiently curved) [39,53] or highly curved like those of SUVs [54].

different folding intermediates could be trapped at different temperatures, when experiments were performed between 2 °C and ~28 °C in bilayers of *di*$C_{18:1}$PC (SUVs). Over this temperature range, *di*$C_{18:1}$PC bilayers are fluid, because *di*$C_{18:1}$PC has a gel-to-liquid crystalline phase transition temperature of ~−18 °C [83]. Three previously unidentified folding intermediates on the pathway of OmpA insertion and folding into lipid bilayers were detected, trapped and characterized by differences in the quenching of their W-fluorescence at different temperatures [38,49]. Folding of wt-OmpA was investigated using positional isomers of lipids carrying two vicinal bromines in the *sn*-2 acyl chains. The vicinal bromines quench fluorescence and the used brominated lipid isomers allowed monitoring the translocation of W residues across the lipid membrane [49]. The positions of the bromines in 1-palmitoyl-2-(4,5-dibromo-)stearoyl-*sn*-glycero-3-phosphocholine (4,5-DiBrPC), in 6,7-DiBrPC, in 9,10-DiBrPC, and in 11,12-DiBrPC are known from X-ray diffraction to be 12.8, 11.0, 8.3, and 6.5 Å from the center of the lipid bilayer [84,85]. The fluorescence quenching profiles observed at defined times after initiation of OmpA folding at a selected temperature were analyzed by distribution analysis [86] and by the parallax method [87] to determine the distance of W residues from the center of the lipid bilayer as a function of time after initiation of insertion and folding at selected temperatures. The first folding intermediate was stable at 2 °C for at least 1 h. In this intermediate, the fluorescent W side-chains were on average located at about 15–16 Å from the center of the lipid bilayer. A second intermediate was isolated at temperatures between 7 and 20 °C. The W residues move 4–5 Å closer to the center of the bilayer at this stage. Subsequently, in an intermediate that is observable at 26–28 °C, the Ws move another 5–10 Å closer to the center of the bilayer. The final (native) structure was observed at higher temperatures chosen for folding experiments. In this structure, the Trps are located on average about 9–10 Å from the bilayer center [49], consistent with the structure of OmpA. The β-barrel domain of wt-OmpA contains 5 W residues (W_7, W_{15}, W_{57}, W_{102}, and W_{143}), while the periplasmic domain does not contain any. These W were later replaced by phenylalanine (F) using site-directed mutagenesis to prepare five different single W mutants, each with one W at one of the five original positions. The time-resolved distance determinations by fluorescence quenching [49] were repeated for each of the five mutants [38]. These experiments showed that the four translocating W residues (W_{15}, W_{57}, W_{102}, and W_{143}) cross the membrane synchronously. The four mutants W_{15}, W_{57}, W_{102}, and W_{143}-OmpA displayed folding intermediates similar to wt-OmpA [49]. In contrast the mutant W_7 did not display structurally distinct folding intermediates in these experiments and remained at a distance of ~10–11 Å in the outer leaflet of the vesicle (which corresponds to the inner leaflet of the OM).

To correlate the synchronous translocation of the β-strands observed in these studies with the formation of the β-barrel, the association of neighboring β-strands during folding of OmpA was investigated in a subsequent study [88]. Based on the OmpA structure, several double mutants of OmpA were designed and prepared by site-directed mutagenesis, each with a single-W, and a single cysteine (C) in the β-barrel domain (Fig. 5A). The W and the C were introduced in two neighboring β-strands oriented toward the hydrocarbon core of the membrane. Replaced residue pairs were either closer to the periplasmic turns (on periplasmic, *cis*-side), or the outer loops (*trans*-side) of the strand. W_nC_m-OmpA mutants containing W at position *n* and C at position *m* along the polypeptide chain were labeled at the C by a nitroxyl spin-label, which is a short-range fluorescence quencher. To monitor association of neighboring β-strands, the proximity between fluorescent W and labeled C was determined in OmpA folding experiments by intramolecular fluorescence quenching [88]. Formation of native β-strand contacts in folding experiments required the lipid membrane. Residues in the *trans*-side of strands β_1, β_2, and β_3, represented by mutants $W_{15}C_{35}$($\beta_1\beta_2$, *trans*) and $W_{57}C_{35}$($\beta_3\beta_2$, *trans*), reached close proximity prior to residues in the amino (β_1)- and carboxy (β_8)-terminal strands as examined for mutants $W_{15}C_{162}$($\beta_1\beta_8$, *trans*) and W_7C_{170}($\beta_1\beta_8$, *cis*). W and C converged slightly faster in $W_{15}C_{162}$($\beta_1\beta_8$, *trans*) than in W_7C_{170}($\beta_1\beta_8$, *cis*). The last folding step was observed for residues at the *cis*-ends of strands β_1 and β_2 for the mutant W_7C_{43}($\beta_1\beta_2$, *cis*). The data also demonstrated that the neighboring β-strands associate upon insertion into the hydrophobic core of the lipid bilayer. Inter- [38,49] and intramolecular [88] site-directed quenching of the W-fluorescence emission of OmpA have been powerful techniques to examine the folding and insertion mechanism of the TM β-barrel of this OMP, leading to a scheme for folding and membrane insertion, which is depicted in Fig. 5. The folding model depicted in Fig. 5 has also been supported by fluorescence energy transfer experiments [89].

3.10. PagP folds and inserts via a tilted transition state

A highly cooperative insertion and folding process has also been reported for PagP [41]. At a high *di*$C_{12:0}$PC/PagP ratio of 3200/1, pH 8, 25 °C, and at a residual urea concentration of 7.6 to 8.8 M urea, a single step for folding of PagP into *di*$C_{12:0}$PC bilayers was reported, while unfolding was a single step process at all urea concentrations (8.5 to 10 M) that were examined, leading to V-shaped chevron plots. In a urea concentration range from 7.6 to 10 M, PagP folding was completely reversible. φ-value analysis [90,91] was used to study the transition

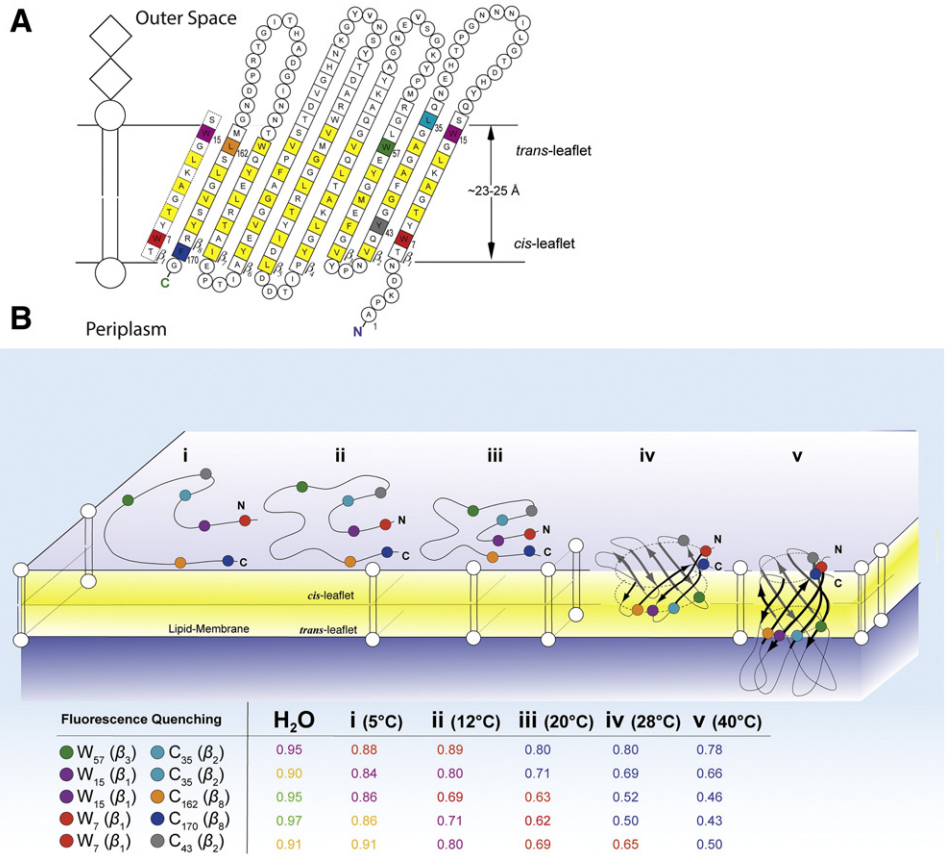

Fluorescence Quenching	H_2O	i (5°C)	ii (12°C)	iii (20°C)	iv (28°C)	v (40°C)
W_{57} (β_3) C_{35} (β_2)	0.95	0.88	0.89	0.80	0.80	0.78
W_{15} (β_1) C_{35} (β_2)	0.90	0.84	0.80	0.71	0.69	0.66
W_{15} (β_1) C_{162} (β_8)	0.95	0.86	0.69	0.63	0.52	0.46
W_7 (β_1) C_{170} (β_8)	0.97	0.86	0.71	0.62	0.50	0.43
W_7 (β_1) C_{43} (β_2)	0.91	0.91	0.80	0.69	0.65	0.50

Fig. 5. Tentative scheme for the folding mechanism of the TMD of OmpA, adapted from Ref. [88]. (A) The primary structure of the polypeptide chain of wt-OmpA (residues 1–171) and its TM topology are shown. For intramolecular fluorescence quenching, all native W were first replaced by F using site-directed mutagenesis on the encoding plasmid DNA. Plasmid was further mutated for the expression and isolation of five single-W, single-C mutants. The prepared single-W, single-C mutants of OmpA were $W_{57}C_{35}$, $W_{15}C_{35}$, $W_{15}C_{162}$, W_7C_{170}, and W_7C_{43}. (B) Tentative scheme for the folding mechanism of the TMD of OmpA. Each of the five OmpA mutants $W_{57}C_{35}$, $W_{15}C_{35}$, $W_{15}C_{162}$, W_7C_{170}, and W_7C_{43} were either labeled with a fluorescence quencher, a nitroxide spin-label, or methylated (to prevent dimerization or modifications of the sidechain). Intramolecular fluorescence quenching was analyzed as the ratio R_Q = fluorescence of the spin-labeled mutant $F(SL\text{-}W_nC_m)$/fluorescence of the methylated mutant $F(Me\text{-}W_nC_m)$. The fluorescence ratios shown in the Table were determined at 330 nm from spectra recorded after 60 min of incubation in water or in presence of DOPC bilayers (SUVs) at the indicated temperatures. The folding scheme was derived from these fluorescence quenching data [88] and earlier studies, in which the membrane insertion of the five W residues of OmpA was analyzed [38,49].

state of PagP folding [41]. φ is the ratio between the change in the free energy of the transition state and the change in the free energy of the folded state after a mutation, relative to the reference state of the unfolded protein. A mutation in a region that is native-like in the transition state will lead to an equal destabilization (or stabilization) of the transition state and the folded state. In this case the mutation is characterized by φ-values close to 1. In contrast, a region that is unfolded in the transition state will lead to a destabilization/stabilization of the folded state only and therefore will display a φ-value close to 0. From kinetic and thermodynamic experiments with 19 point mutants of PagP, chosen to destabilize PagP [41], φ-values were obtained and mapped on the structure of PagP (Fig. 6). These data suggest a tilted insertion of PagP

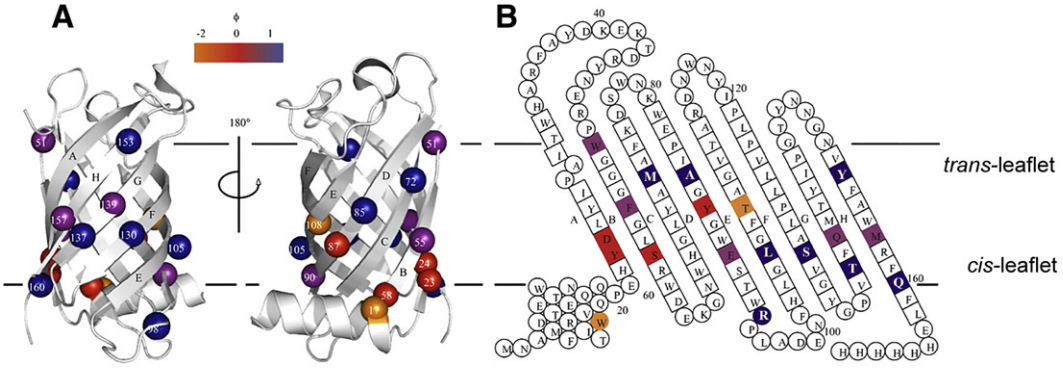

Fig. 6. φ-values determined from kinetic and thermodynamic analysis of PagP folding into $diC_{12:0}PC$ bilayers. φ-values of PagP are mapped onto a ribbon representation of PagP (left) and onto a topology model (right). Regions with φ-values close to 0 indicate less structured regions in the transition state and are shown in red ($\varphi < 0.3$), regions with φ-values close to 1 indicate structured regions in the transition state and are shown in blue. Intermediate φ-values, ranging from 0.3 to 0.5, and φ-values less than 1 are indicated in purple and in orange, respectively.
Adapted from Ref. [41].

into thin and flexible *di*$C_{12:0}$PC bilayers. A tilted insertion has also be predicted by simulations [92], although these were performed with *di*$C_{16:0}$PC bilayers, which in experiments do not favor insertion and folding of OMPs like OmpA, as they are present in the gel-phase. The transition state is characterized by native-like structure in the trans-side of the forming β-barrel and in the carboxy-terminal β-strands. Since folding of OMPs like PagP and OmpA into thin and flexible bilayers of *di*$C_{12:0}$PC is faster than folding into bilayers of *di*$C_{18:1}$PC (SUVs), partly membrane inserted intermediates were not observed for PagP. At the conditions used in these experiment, the unfolded form of PagP is membrane-adsorbed. However, the properties of the transition state found for PagP reflect many of the properties described for membrane-bound intermediates of insertion and folding of OmpA into thicker bilayers of *di*$C_{18:1}$PC [38,49,88].

3.11. Studies with other OMPs

Studies with another TM β-barrel, FomA from *F. nucleatum*, predicted to form a 14 stranded TM β-barrel [93,94], suggest that this OMP and likely other OMPs share most of the principles of lipid bilayer insertion and folding observed for OmpA and PagP, including the dependence on bilayer thickness and temperature (in the range between 2 and 40 °C) [30,32] and irrespective of the size of their barrel domain. To date, the 19-stranded β-barrel of the human VDAC is the largest TM β-barrel successfully refolded into lipid bilayers, in this case *di*$C_{12:0}$PC and *di*$C_{14:0}$PC (LUVs) [20]. OMPs investigated later, like the 8-stranded barrels OmpX and OmpW, the 10-stranded OmpT, the 12-stranded OmpLA, the 14-stranded FadL, the 16-stranded BamA and the trimeric 16-stranded OmpF, also appear to fold more efficiently into thinner bilayers of LUVs and smaller vesicles [42,37]. The investigation by Burgess et al. [42] on OMPs from *E. coli* also confirmed that folding is most efficient at basic pH, as can be expected from an increased net-charge and better solubility at pH ≫ pI [7] for *E. coli* OMPs. The vast majority of OMPs from *E. coli* are characterized by a pI ~ 5 to 6 (see Table 1). However, the 8-stranded barrels OmpA, OmpX, PagP, and OmpW folded with different rates, indicating that the size of the barrel alone is not the only parameter affecting folding rates [42]. Although some folding conditions were shared among the proteins, a single folding condition could not be identified. This likely is a consequence of the aggregation of OMPs due to differences in their hydrophobic nature. Aggregation will depend on local and overall hydrophobicity of individual proteins, the presence of a soluble domain like in OmpA, which is independently folded even in the absence of detergents or lipids [28,95,96], and on the selected experimental conditions. However, in cells the aggregation is prevented by molecular chaperones [97] and it can be anticipated that most TM β-barrel proteins follow the same principles of insertion and folding into membranes when aggregation reactions are suppressed.

A highly basic pH was also favorable for insertion and folding of two OMPs from *Neisseria gonorrhea*, the opacity associated proteins Opa_{60} and Opa_{50} [98]. Typical for OMPs from *Neisseria*, these proteins have a much higher isolelectric point (pI ~9.6 for Opa_{60} and pI 9.9 for Opa_{50}). Aggregation was still greatly reduced at pH 10 and above and insertion was improved in thinner bilayers of lipids with shorter hydrophobic chains. The study also demonstrated that insertion was retarded by ether-lipids or unsaturated lipids and the authors propose roles for the membrane surface potential and the dipole potential in driving folding and insertion of OMPs [98].

4. Folding of β-barrel membrane proteins into lipid bilayers in the presence of chaperones and folding facilitators

4.1. Transport and folding of OMPs in cells

After their synthesis in the cytoplasm, OMPs are translocated across the inner membrane in an unfolded form by the SecYEG translocation channel. In the periplasm, a signal peptidase cleaves off the signal sequence before the OMPs are transported through the periplasm and inserted into the OM by the BAM complex (Fig. 7).

4.2. Periplasmic chaperones

Periplasmic chaperones for OMPs, like Skp or the survival factor A (SurA), were discovered and characterized by genetic, microbiological, biochemical, and structural studies (for reviews see *e.g.*, [97,99–102]). Skp and SurA have been identified as the main periplasmic chaperones

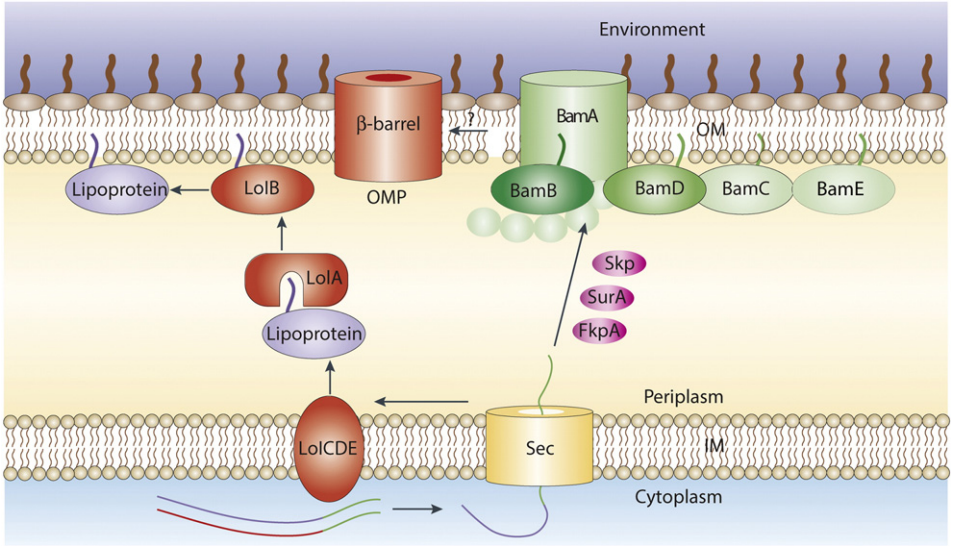

Fig. 7. After their synthesis in the ribosomes of the cytoplasm, OMPs are transported in unfolded form across the cytoplasmic membrane *via* the SecYEG translocon. A signal peptidase cleaves off the signal sequence. Periplasmic chaperones like Skp or SurA keep OMPs soluble before these bind and insert into the OM. OMPs insert and fold into the OM *via* the Barrel Assembly Machinery (BAM) complex. The BAM complex is composed of five proteins: The TMP BamA and four peripheral proteins BamB, BamC, BamD, and BamE. The BAM proteins BamB, BamC, BamD, and BamE contain an amino-terminal C, which carries a lipid anchor, a thioether-linked diacylglyceryl group and a palmitoyl chain at the amino terminus. A detailed topology of the BAM-complex in membranes has not yet emerged. The BAM complex is composed of two sub-complexes, BamAB and BamCDE [147,150]. Lipoproteins are translocated to the OM *via* the LOL pathway [172].
Adapted from Ref. [173].

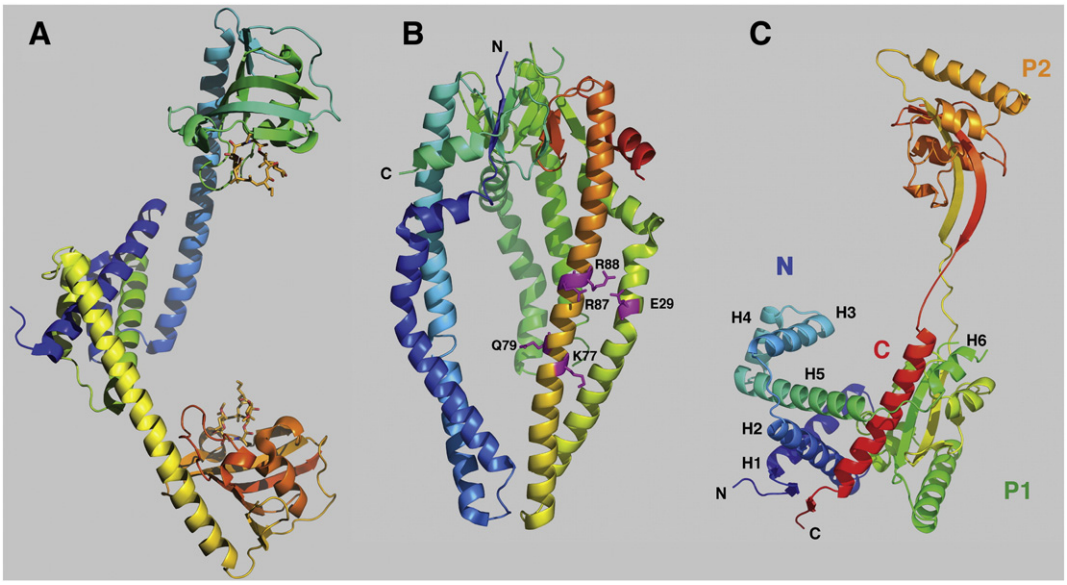

Fig. 8. Crystal structures of periplasmic chaperones. (A) Crystal structure of the V-shaped FkpA dimer in complex with the immunosuppressant FK506 (PDB entry 1Q6I) [114]. Each of the 2 monomers consists of the N-domain, composed of three α-helices (formed by residues 19–43, 51–62, and 70–111, respectively), which functions as a chaperone. For monomer 1, this domain is shown in blue color, for monomer 2 in yellow and in light green. The C-domains of the two monomers are indicated dark green (C-Dm 1) and in orange color (C-Dm 2) and contain the peptidyl-prolyl cis/trans isomerase (PPIase) activity [114]. (B) Crystal structure of the Skp trimer (PDB entries 1SG2 [110] and 1U2M [111]). The Skp trimer consists of a tightly packed 9-stranded β-barrel that is surrounded by C-terminal α-helices of the three subunits that point away from the barrel in form of tentacles that are about 65 Å long. These tentacles form a cavity that may take up the unfolded OMP. The outside surface of the helical domain of Skp is highly basic. Each monomer of the trimeric Skp may contain an LPS binding site [111] compatible with a previously identified LPS binding motif [174] and formed by K77, R87, R88. (C) Crystal structure of Survival Factor A, SurA (PDB entry 1M5Y, [112]). The N-terminal domain (N) is composed of the α-helices H1 to H6 (residues 1 to 148) and connected to peptidyl-proly *cis/trans* isomerase (PPI) domain P1 (residues 149 to 260). The P2 domain (residues 261 to 369) connects the P1 domain to the C-terminal domain C (residues 370 to 428, colored in red). Thus, the N and C domain together constitute a compact core, which is traversed by a broad deep crevice of about 50 Å in length, suggesting a polypeptide binding-site. The active PPIase domain 2 (P2) is tethered to this core by two extended peptide segments. It has been demonstrated that a mutant, SurAN(-Ct), which does not contain the two PPIase domains and is composed of the N and C domains only, functions like a chaperone [175]. This SurA "core domain" has been proposed to bind the tripeptide motif aromatic-random-aromatic, which is prevalent in the aromatic girdles of β-barrel membrane proteins [123]. Images of the structures were created with Pymol [171].
Adapted from Ref. [97].

in the assembly pathway of OMPs. In addition, FkpA [103] might have a role in the assembly of OMPs, as shown recently for LptD [104]. Skp was found as the predominant protein retained by an affinity column with sepharose-bound unfolded outer membrane porin OmpF [105]. In *E. coli*, expression of periplasmic chaperones is under control of either the σ^E [106,107] or the two-component CpxA/CpxR [108,109] stress-response system and upregulated when misfolded OMPs accumulate in the periplasm. Periplasmic chaperones are key factors to prevent aggregation and misfolding of bacterial OMPs [97,99–102] and high-resolution structures have been solved *e.g.*, for Skp [110,111], SurA [112,113], and FkpA [114] (Fig. 8). Deletion of the genes *skp* [105,115] or *surA* [103,116,117], resulted in reduced concentrations of OMPs in the OM, providing further evidence that these periplasmic proteins serve as molecular chaperones in the assembly pathway of OMPs. Later evidence indicated SurA and Skp function in parallel chaperone pathways of OMP transport [118]. Null mutations in *skp* and *surA* as well as in *degP* (a gene encoding the periplasmic protease DegP) and *surA* resulted in synthetic phenotypes. The *skp surA* null combination had a bacteriostatic effect and led to filamentation, while the *degP surA* null combination was bactericidal. Based on SurA depletion studies indicating a strong reduction in the density of the OM and on observations of a direct interaction of SurA with BamA *in vivo*, it has been suggested that the SurA chaperone pathway is the primary pathway for OMP delivery to the outer membrane and that Skp/DegP function to rescue off-pathway intermediates of OMPs [119]. A later article [120] suggested only a subset of OMPs, eight out of 23 that were examined, are affected in the SurA pathway. For Skp, a systematic investigation of the substrate profile with periplasmic cell extract and MALDI-TOF mass spectrometry indicated more than 30 other interacting proteins, in particular from the OM, like Tsx, BtuB, FepA, and FadL, but also from the periplasm, like MalE and OppA, demonstrating a broad substrate spectrum [121]. Biochemical experiments indicated a much higher binding affinity of OMPs for Skp [65,73] than for SurA [122,123] from *E. coli*. For *Neisseria meningitidis*, an important role in the assembly of OMPs was reported for Skp but not for SurA [115].

4.3. Skp-assisted folding of OmpA into lipid bilayers

The first study describing folding of β-barrel TMPs into lipid bilayers in the presence of a molecular chaperone, Skp, was performed for OmpA [65]. Skp facilitated folding of OmpA into bilayers composed of a mixture of $di C_{18:1}$PC, 1,2-dioleoyl-*sn*-glycero-3-phosphoethanolamine ($di C_{18:1}$PE), and 1,2-dioleoyl-*sn*-glycero-3-phosphoglycerol ($di C_{18:1}$PG) at a ratio of 5:3:2, but only when the negatively-charged LPS was also present in small stoichiometric amounts, 3 to 7 LPS per Skp [65]. Binding experiments indicated a nanomolar affinity of complex formation and a stoichiometry of 3:1 for the binding of Skp to OmpA.

Later studies showed that Skp is present as a trimer, in solution [124] as in the crystal structure [110,111]. For the Skp trimer, a stoichiometry of 1:1 and high binding affinities were reported for complexes with OmpG and BamA from *E. coli*, for FomA from *F. nucleatum*, and for NalP from *N. meningitidis*. In contrast, Skp did not bind to a eukaryotic OMP, hVDAC1 from human mitochondria [73]. The binding affinity of Skp to OmpG and OmpA was reduced at high ionic strength and at pH above the pI of Skp (Fig. 2). Skp shielded the fluorescent W residues from fluorescence quenching [73], indicating binding included the TM strands, where the five W of OmpA are located. The β-barrel-domain of OmpA was shown to bind in unfolded form [65] in the cavity of Skp [95,125,126], populating a dynamic conformational ensemble with structural interconversion rates on the submillisecond timescale [126]. W-scanning mutagenesis and W-fluorescence spectroscopy of unfolded OmpA in aqueous solution after urea-dilution indicated that the loops

and turns form the surface of the hydrophobically collapsed barrel domain of OmpA, while the strand regions are less exposed to water [125]. The addition of Skp increased the fluorescence of all OmpA mutants, demonstrating binding of Skp to the entire β-barrel domain and suggesting OmpA is bound inside the Skp tentacle domain. Skp bound the TMD of OmpA asymmetrically, displaying much stronger interactions with strands β_1 to β_3 in the N-terminus than with strands β_5 to β_7 in the C-terminus. In contrast, a similar asymmetry was not observed for the outer loops and the periplasmic turns of the TMD of OmpA. The W-fluorescence profiles obtained before and after addition of Skp suggest that the relative surface exposure of the W-residues does not change much upon Skp binding. The addition of five negatively charged LPS per one preformed $Skp_3 \cdot W_n$-OmpA complex released the C-terminal loops l_2, l_3, and l_4 of the TMD of OmpA from the complex, while its periplasmic turn regions remained bound to Skp [125].

4.4. Skp facilitates insertion and folding of OMPs into lipid bilayers with a negative electrostatic surface potential

A more detailed study on the role of Skp in the folding of OmpA into lipid bilayers demonstrated that bilayers with a negative electrostatic surface potential are necessary for the efficient release of OmpA from complexes with Skp [66]. Skp in fact strongly inhibited folding into bilayers of phosphatidylcholine, acting as a holdase. Even the additional presence of LPS had only a weak effect on the function of Skp in the presence of bilayers composed of phosphatidylcholine only. Folding of OmpA was completely inhibited in bilayers composed of a mixture of $di C_{18:1}$PC and $di C_{18:1}$PE (7:3), an effect attributed to the presence of phosphatidylethanolamine. This was observed for urea-unfolded OmpA and for Skp-bound OmpA and regardless of the presence of LPS [66]. In contrast, when lipid bilayers also contained phosphatidylglycerol, Skp facilitated folding, despite the presence of 30 mol-% $di C_{18:1}$PE. Folding of Skp-bound OmpA was facilitated either into binary mixtures of phosphatidylglycerol with phosphatidylcholine at a ratio of 7:3 or in ternary mixtures composed of $di C_{18:1}$PC, $di C_{18:1}$PE, $di C_{18:1}$PG at a ratio of 5:3:2 [66] (Fig. 9A). The additional presence of LPS also contributed to a faster kinetics, but this effect was lower than the effect observed by addition of ≥20% phosphatidylglycerol [66]. In cells, a role of LPS in the release of OMPs from complexes with Skp appears unlikely, since LPS is translocated across the periplasm *via* seven LPS transport (Lpt) proteins [127]. LPS and phosphatidylglycerol are both negatively charged. Electrostatic interactions are important for the formation of $Skp_3 \cdot$OMP complexes and studies demonstrated they are equally important for the release of OMPs from complexes with Skp at the membrane surface [66]. In fact, the effect of LPS on the release of OmpA from complexes with Skp could be circumstantial, caused by (unspecific) interactions of the negative charges of the phosphate groups of LPS with $Skp_3 \cdot$OMP complexes. The study by Patel et al. instead suggests the release of the OMP is triggered by the negative surface charges of lipid bilayers containing phosphatidylglycerol, as illustrated in Fig. 9A. Apparently the main driving force for the release of OMPs from complexes with Skp are electrostatic interactions rather than very specific interactions of Skp with lipids like LPS or phosphatidylglycerol. In fact, release of OMPs from complexes with Skp was also observed in the absence of negatively charged lipids but in the presence of negatively charged protein, namely BamA from *E. coli* [62]. Interestingly the kinetics of OmpA folding in the

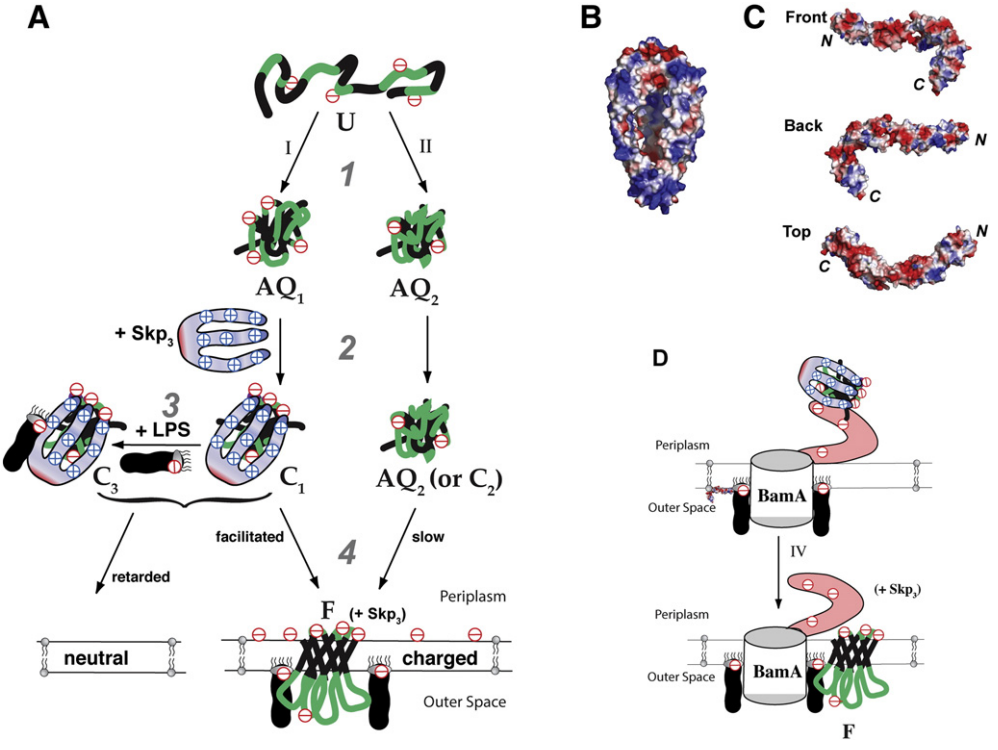

Fig. 9. Skp delivers OmpA to the membrane *via* charge–charge interactions. (A), (*1*) Unfolded OmpA in 8 M urea is negatively charged above pH ~ 5.5. Polar segments of the TMD of OmpA are colored in green, TM segments in black. Upon urea dilution OmpA collapses into more or less compact aqueous forms (AQ_1, AQ_2) with charged or polar residues on the surface and hydrophobic residues buried inside. Titrations between aqueous forms may depend on parameters like pH, membrane surface potential, *etc*. These forms of OmpA fold in parallel processes into lipid bilayers. Experimentally, a fast (I) and a slow (II) process have been distinguished [66]. (*2*) Positively charged Skp_3 binds to AQ_1 (and possibly also AQ_2) forming stable complexes (C_1, C_2) and preventing further misfolding. (*3*) In model experiments, Skp_3 · OmpA complexes bound negatively charged LPS at low stoichiometric amounts and formed complexes C_3. (*4*) Electrostatic interactions between positive charges of Skp_3 of the complexes C_1, C_2 (or C_3) and negatively charged membranes lead to OmpA release from complexes and to its insertion and folding to the folded form (F) in the membrane. Folding of OmpA from complexes into membranes without electrostatic surface potential is retarded, leading to reduced yields. (B) Structure of the Skp trimer (*1sg2* and *1u2m*) [110,111], which forms a large dipole. Positive residues (colored in blue) cover the surface of the Skp tentacles down to their tips. (C) Structure of the amino-terminal domain (residues 23–347) of BamA (YaeT, Omp85) (*3efc*) of *E. coli*. D The surface of this domain contains several patches with a negative surface potential (colored in red). The domain extends from the membrane surface into the periplasm and may bind $Skp_3 \cdot$OMP complexes through electrostatic attraction.
Adapted from Refs. [62,66].

presence of Skp could be well described by fits of Eqs. (3) and (4), regardless of the lipid membranes, into which OmpA was folded [66]. The analysis demonstrated that the contribution of the faster folding phase correlates with the pH-titration of OmpA shown in Fig. 2A. In the presence of Skp and for folding of OmpA into bilayers containing *di*$C_{18:1}$PC only, the contribution of the faster process was much decreased, consistent with the observed inhibitory effect of Skp.

Very similar observations as described for the Skp-assisted folding of OmpA into bilayers of *di*$C_{18:1}$PC, *di*$C_{18:1}$PE, and *di*$C_{18:1}$PG [65,66] were made by McMorran et al. for insertion/folding of PagP into thinner bilayers of either *di*$C_{12:0}$PC or mixtures of *di*$C_{12:0}$PC and 1,2-dilauryl-*sn*-glycero-3-phosphoglycerol (*di*$C_{12:0}$PG) (8:2) [128]. Skp showed holdase activity against his-tagged PagP, which is highly prone to aggregation. In the same study McMorran et al. also showed that SurA does not affect folding of PagP into lipid bilayers.

4.5. Insertion and folding of OmpT into bilayers of lipids from E. coli is mediated by the BAM complex

A wide range of reports have demonstrated that folding of β-barrel TMPs into detergent micelles, lipid bilayers or amphipols is spontaneous and does not require folding machinery or energy sources like ATP. In cells, the insertion of OMPs into the OM is still spontaneous (there is no ATP in the periplasm), but it requires the presence of a protein complex. This is not surprising, as the main phospholipid of the periplasmic leaflet of the OM is phosphatidylethanolamine [129,130], a lipid known to inhibit folding and insertion of OMPs like OmpA from complexes with periplasmic chaperones [66]. Genetic studies have shown that the assembly of OMPs of bacteria, mitochondria and chloroplasts into OMs requires the BAM complex see *e.g.*, [131–134]. For reviews of the BAM complex, see *e.g.*, [135–143] and references therein. In *E. coli*, the BAM complex is composed of one TM protein, BamA (also called YaeT or Omp85) [134,144,145] and of four peripherally anchored lipoproteins, BamB (originally called YfgL), BamC (NlpB), BamD (YfiO), and BamE (SmpA). Only BamA and BamD are essential proteins, but the depletion of BamB in a *bamE* deletion strain is also lethal to cells [146]. Deleting any protein of the complex results in assembly defects of the OM [131, 133,146]. In an elegant approach, Hagan et al. showed that the BAM complex can be reconstituted into *E. coli* lipid extract in functional form from subcomplexes [147]. The subcomplexes BamA,B and BamC,D,E were expressed separately, isolated in the presence of dodecylmaltoside (BamC,D,E) or *N*-lauryl, *N*, *N*-dimethylamine-*N*-oxide (BamA,B), and reconstituted into *E. coli* lipids by detergent dilution. In blue-native-PAGE, the reconstituted BAM-complex migrated at an apparent molecular mass corresponding to a ratio of BamA:B:C:D of 1:1:1:1, while the exact stoichiometry in regard to the comparably small BamE could not be determined. To monitor its insertion and folding, OmpT was first denatured by urea and then kept soluble by SurA [147]. Incubation of unfolded OmpT in the presence of the reconstituted BAM-complex in bilayers of *E. coli* lipids led to the typical shift in the electrophoretic migration of OmpT and it also resulted in activity of OmpT as a protease. As indicated in the activity assays, OmpT regained activity in the simultaneous presence of all proteins of the BAM complex. Much lower activity of OmpT was developed when the lipid vesicles contained only subcomplexes, BamA,B or BamA,C,D,E [147] indicating that although not essential, BamB is important for the assembly of OmpT in the presence of SurA. Demonstration of functional insertion of OmpT into liposomes containing the reconstituted BAM-complex depended on the simultaneous presence of SurA. Although SurA is not essential for cell survival, it may be important for OmpT insertion into the OM.

4.6. Effects of pre-inserted integral proteins on insertion and folding of OmpA into lipid bilayers

As summarized above, processes of folding and insertion of β-barrel TMPs into lipid bilayers and their kinetics are dependent on the properties of the lipid bilayer. To examine, how integral membrane proteins influence insertion and folding of β-barrel TMPs into lipid bilayers is both, of physicochemical interest and important for the characterization of protein assembly factors, to distinguish specific from unspecific effects. Therefore, folding of OmpA was examined into two different kinds of proteoliposomes [62], containing either the pre-inserted BamA of the BAM complex from *E. coli* or FomA from *F. nucleatum*, which is not part of any folding machinery. Four different preformed membranes of *di*$C_{12:0}$PC bilayers were prepared to compare the kinetics of folding and insertion of OmpA. These were proteoliposomes containing either wt-BamA, TMD-BamA, or FomA and pure liposomes of *di*$C_{12:0}$PC. BamA from *E. coli* (88 kDa), is composed of a C-terminal TMD, that forms a β-barrel (~385 residues), and of an about equally sized N-terminal periplasmic domain (PD). The PD consists of five polypeptide-transport-associated (POTRA) subdomains [148–152] (residues 1–405). The proteoliposomes were prepared by folding the unfolded β-barrel proteins into preformed lipid vesicles because this leads to proteoliposomes, in which the inserted TMPs have a defined orientation [28,62]. The incorporation of each of the proteins into lipid bilayers accelerated folding of OmpA in comparison to the pure lipid bilayer. However, at an ~3-fold molar excess of OmpA, the kinetics of OmpA folding and insertion was 2 times faster for bilayers containing wt-BamA than for bilayers containing FomA during the first 5 min after initiation of folding [62]. Apparently, the simple presence of a membrane protein already has a strong impact on the properties of a *di*$C_{12:0}$PC bilayer, resulting in significantly faster folding rates of unfolded β-barrels. A pre-inserted TMP like FomA alters the surface properties of the membrane in its direct vicinity such as the hydrophobic thickness of the membrane [58,60] and presents a lipid protein interface that is likely to affect insertion of unfolded TMPs.

4.7. BamA cancels the inhibiting effect of PE partly and mediates folding of Skp bound OMPs

Interestingly the incorporation of BamA into lipid bilayers containing phosphatidylethanolamine (*di*$C_{12:0}$PE) greatly weakened the inhibiting effect of phosphatidylethanolamine on the folding of OmpA [62,66], as later confirmed in another study [153]. Patel et al. [62] demonstrated that BamA facilitated folding of OmpA from a complex with the periplasmic chaperone Skp into bilayers composed of phosphatidylethanolamine and phosphatidylcholine, while folding was inhibited in the absence of BamA. This study indicated an interaction of Skp·OmpA complexes with BamA and suggests that Skp delivers OMPs to the BAM complex also in cells, as first suggested in Ref. [66] and confirmed later [62] (Fig. 9). Interestingly, the soluble periplasmic domain of BamA contains several patches of negatively charged residues (Fig. 9C) and may be instrumental in the release of OMPs from complexes with Skp for insertion into the membrane (Fig. 9D). BamA seems to facilitate folding of client OMPs only when the signature sequence of the C-terminal β-strand is present in the unfolded client OMP [153–155].

4.8. Peripheral lipoproteins BamB and BamD are instrumental and sufficient to insert BamA into bilayers of E. coli lipid extracts

The peripheral membrane proteins BamB and BamD have recently been shown to result in insertion and folding of urea-unfolded FLAG-tagged BamA into lipid bilayers of *E. coli* lipid extract [156]. The presence of a periplasmic chaperone was not required. Interestingly, the BamC,D,E subcomplex, was able to insert unfolded BamA into bilayers of *E. coli* lipid more efficiently than preinserted non-tagged BamA, indicating that insertion of BamA does not require BamA to be already present in the bilayer. However, the BamC,D,E subcomplex was not sufficient to insert FLAG-tagged OmpA, which instead required preinserted BamA in addition. Insertion of FLAG-tagged BamA was also successful for variants, in which the POTRA5 domain of BamA was replaced by other POTRA domains, effectively eliminating the binding site for the

BamC,D,E subcomplex in BamA. This study demonstrated further that BamB and BamD individually facilitate the insertion of FLAG-tagged BamA into lipid vesicles of *E. coli*. Interestingly, the β-barrel of BamA is 16-stranded and therefore much larger than the TMD of OmpA. The study [156] therefore also suggests, that the TMD of BamA is in principle not required to insert even a larger 16-stranded β-barrel into a lipid bilayer composed of an *E. coli* lipid extract. This suggests that the β-barrel is largely formed in the periplasmic part of the BAM-complex at a polar/apolar interface similar to the observations made for insertion and folding into pure lipid bilayers.

5. Perspectives

Although investigations on membrane insertion and folding of β-barrel TMPs into lipid membranes have made much progress over the past decades, a lot of work is still required to fully understand the relations between outer membrane protein primary structure and the sequence of folding events leading to the three-dimensional native fold. This applies to both, assisted and unassisted folding and insertion. Clearly protein–lipid interactions play a key-role in driving membrane proteins into lipid bilayers in the absence of protein folding machinery, likely as a consequence of the hydrophobic effect. Similarly protein–protein interactions and the hydrophobic effect likely play a role in assisted membrane protein folding. The folding machinery of the cell is complex and while structures of the components of the machinery have become available, the biophysical functions of the individual proteins are less clear and need to be addressed in future studies among numerous other topics in this area of research.

Transparency document

The Transparency document associated with this article can be found in the version.

Acknowledgements

Work performed in the author's laboratory was funded by the Deutsche Forschungsgemeinschaft (DFG), the University of Konstanz and the University of Kassel.

References

[1] S.H. White, W.C. Wimley, Membrane protein folding and stability: physical principles, Annu. Rev. Biophys. Biomol. Struct. 28 (1999) 319–365.
[2] E. van den Brink-van der Laan, V. Chupin, J.A. Killian, B. de Kruijff, Stability of KcsA tetramer depends on membrane lateral pressure, Biochemistry 43 (2004) 4240–4250.
[3] H. Hong, L.K. Tamm, Elastic coupling of integral membrane protein stability to lipid bilayer forces, Proc. Natl. Acad. Sci. U. S. A. 101 (2004) 4065–4070.
[4] J.U. Bowie, Solving the membrane protein folding problem, Nature 438 (2005) 581–589.
[5] J.-L. Popot, D.M. Engelman, Helical membrane protein folding, stability, and evolution, Annu. Rev. Biochem. 69 (2000) 881–922.
[6] M. Heyden, J.A. Freites, M.B. Ulmschneider, S.H. White, D.J. Tobias, Assembly and stability of α-helical membrane proteins, Soft Matter 8 (2012) 7742–7752.
[7] J.H. Kleinschmidt, Folding kinetics of the outer membrane proteins OmpA and FomA into phospholipid bilayers, Chem. Phys. Lipids 141 (2006) 30–47.
[8] G. von Heijne, Y. Gavel, Topogenic signals in integral membrane proteins, Eur. J. Biochem. 174 (1988) 671–678.
[9] C. Dong, K. Beis, J. Nesper, A.L. Brunkan-Lamontagne, B.R. Clarke, C. Whitfield, J.H. Naismith, Wza the translocon for *E. coli* capsular polysaccharides defines a new class of membrane protein, Nature 444 (2006) 226–229.
[10] G.E. Schulz, The structure of bacterial outer membrane proteins, Biochim. Biophys. Acta 1565 (2002) 308–317.
[11] W.C. Wimley, The versatile β-barrel membrane protein, Curr. Opin. Struct. Biol. 13 (2003) 404–411.
[12] M. Schweizer, I. Hindennach, W. Garten, U. Henning, Major proteins of the *Escherichia coli* outer cell envelope membrane. Interaction of protein II with lipopolysaccharide, Eur. J. Biochem. 82 (1978) 211–217.
[13] U. Henning, I. Sonntag, I. Hindennach, Mutants (ompA) affecting a major outer membrane protein of *Escherichia coli* K12, Eur. J. Biochem. 92 (1978) 491–498.
[14] K. Dornmair, H. Kiefer, F. Jähnig, Refolding of an integral membrane protein. OmpA of *Escherichia coli*, J. Biol. Chem. 265 (1990) 18907–18911.
[15] J.H. Kleinschmidt, M.C. Wiener, L.K. Tamm, Outer membrane protein A of *E. coli* folds into detergent micelles, but not in the presence of monomeric detergent, Protein Sci. 8 (1999) 2065–2071.
[16] D. Debnath, K.L. Nielsen, D.E. Otzen, In vitro association of fragments of a β-sheet membrane protein, Biophys. Chem. 148 (2010) 112–120.
[17] D.E. Otzen, K.K. Andersen, Folding of outer membrane proteins, Arch. Biochem. Biophys. 531 (2013) 34–43.
[18] R. Koebnik, In vivo membrane assembly of split variants of the *E. coli* outer membrane protein OmpA, EMBO J. 15 (1996) 3529–3537.
[19] S.K. Buchanan, Overexpression and refolding of an 80-kDa iron transporter from the outer membrane of *Escherichia coli*, Biochem. Soc. Trans. 27 (1999) 903–908.
[20] B. Shanmugavadivu, H.J. Apell, T. Meins, K. Zeth, J.H. Kleinschmidt, Correct folding of the β-barrel of the human membrane protein VDAC requires a lipid bilayer, J. Mol. Biol. 368 (2007) 66–78.
[21] H. Engelhardt, T. Meins, M. Poynor, V. Adams, S. Nussberger, W. Welte, K. Zeth, High-level expression, refolding and probing the natural fold of the human voltage-dependent anion channel isoforms I and II, J. Membr. Biol. 216 (2007) 93–105.
[22] D.C. Bay, J.D. O'Neil, D.A. Court, Two-step folding of recombinant mitochondrial porin in detergent, Biophys. J. 94 (2008) 457–468.
[23] S.R. Maurya, R. Mahalakshmi, Modulation of human mitochondrial voltage-dependent anion channel 2 (hVDAC-2) structural stability by cysteine-assisted barrel–lipid interactions, J. Biol. Chem. 288 (2013) 25584–25592.
[24] J.-L. Popot, Folding membrane proteins in vitro: a table and some comments, Arch. Biochem. Biophys. 564 (2014) 314–326.
[25] A. Rath, M. Glibowicka, V.G. Nadeau, G. Chen, C.M. Deber, Detergent binding explains anomalous SDS-PAGE migration of membrane proteins, Proc. Natl. Acad. Sci. U. S. A. 106 (2009) 1760–1765.
[26] H. Vogel, F. Jähnig, Models for the structure of outer-membrane proteins of *Escherichia coli* derived from Raman spectroscopy and prediction methods, J. Mol. Biol. 190 (1986) 191–199.
[27] N.A. Rodionova, S.A. Tatulian, T. Surrey, F. Jähnig, L.K. Tamm, Characterization of two membrane-bound forms of OmpA, Biochemistry 34 (1995) 1921–1929.
[28] T. Surrey, F. Jähnig, Refolding and oriented insertion of a membrane protein into a lipid bilayer, Proc. Natl. Acad. Sci. U. S. A. 89 (1992) 7457–7461.
[29] T. Surrey, F. Jähnig, Kinetics of folding and membrane insertion of a β-barrel membrane protein, J. Biol. Chem. 270 (1995) 28199–28203.
[30] J.H. Kleinschmidt, L.K. Tamm, Folding intermediates of a β-barrel membrane protein. Kinetic evidence for a multi-step membrane insertion mechanism, Biochemistry 35 (1996) 12993–13000.
[31] A. Arora, D. Rinehart, G. Szabo, L.K. Tamm, Refolded outer membrane protein A of *Escherichia coli* forms ion channels with two conductance states in planar lipid bilayers, J. Biol. Chem. 275 (2000) 1594–1600.
[32] C.L. Pocanschi, H.-J. Apell, P. Puntervoll, B.T. Høgh, H.B. Jensen, W. Welte, J.H. Kleinschmidt, The major outer membrane protein of *Fusobacterium nucleatum* (FomA) folds and inserts into lipid bilayers via parallel folding pathways, J. Mol. Biol. 355 (2006) 548–561.
[33] V. Kräutler, S. Hiller, P.H. Hünenberger, Residual structure in a peptide fragment of the outer membrane protein X under denaturing conditions: a molecular dynamics study, Eur. Biophys. J. 39 (2010) 1421–1432.
[34] V. Visudtiphole, M.B. Thomas, D.A. Chalton, J.H. Lakey, Refolding of *Escherichia coli* outer membrane protein F in detergent creates LPS-free trimers and asymmetric dimers, Biochem. J. 392 (2005) 375–381.
[35] K.K. Andersen, H. Wang, D.E. Otzen, A kinetic analysis of the folding and unfolding of OmpA in urea and guanidinium chloride: single and parallel pathways, Biochemistry 51 (2012) 8371–8383.
[36] J.E. Kim, G. Arjara, J.H. Richards, H.B. Gray, J.R. Winkler, Probing folded and unfolded states of outer membrane protein a with steady-state and time-resolved tryptophan fluorescence, J. Phys. Chem. B 110 (2006) 17656–17662.
[37] T. Surrey, A. Schmid, F. Jähnig, Folding and membrane insertion of the trimeric β-barrel protein OmpF, Biochemistry 35 (1996) 2283–2288.
[38] J.H. Kleinschmidt, T. den Blaauwen, A. Driessen, L.K. Tamm, Outer membrane protein A of *E. coli* inserts and folds into lipid bilayers by a concerted mechanism, Biochemistry 38 (1999) 5006–5016.
[39] J.H. Kleinschmidt, L.K. Tamm, Secondary and tertiary structure formation of the β-barrel membrane protein OmpA is synchronized and depends on membrane thickness, J. Mol. Biol. 324 (2002) 319–330.
[40] G.H. Huysmans, S.E. Radford, D.J. Brockwell, S.A. Baldwin, The N-terminal helix is a post-assembly clamp in the bacterial outer membrane protein PagP, J. Mol. Biol. 373 (2007) 529–540.
[41] G.H. Huysmans, S.A. Baldwin, D.J. Brockwell, S.E. Radford, The transition state for folding of an outer membrane protein, Proc. Natl. Acad. Sci. U. S. A. 107 (2010) 4099–4104.
[42] N.K. Burgess, T.P. Dao, A.M. Stanley, K.G. Fleming, β-barrel proteins that reside in the *Escherichia coli* outer membrane in vivo demonstrate varied folding behavior in vitro, J. Biol. Chem. 283 (2008) 26748–26758.
[43] S.R. Maurya, D. Chaturvedi, R. Mahalakshmi, Modulating lipid dynamics and membrane fluidity to drive rapid folding of a transmembrane barrel, Sci. Rep. 3 (2013) 1989.
[44] C.L. Pocanschi, T. Dahmane, Y. Gohon, F. Rappaport, H.-J. Apell, J.H. Kleinschmidt, J.-L. Popot, Amphipathic polymers: tools to fold integral membrane proteins to their active form, Biochemistry 45 (2006) 13954–13961.
[45] A.C. Leney, L.M. McMorran, S.E. Radford, A.E. Ashcroft, Amphipathic polymers enable the study of functional membrane proteins in the gas phase, Anal. Chem. 84 (2012) 9841–9847.
[46] C.L. Pocanschi, J.-L. Popot, J.H. Kleinschmidt, Folding and stability of outer membrane protein A (OmpA) from *Escherichia coli* in an amphipathic polymer, amphipol A8–35, Eur. Biophys. J. 42 (2013) 103–118.

[47] J.H. Kleinschmidt, J.L. Popot, Folding and stability of integral membrane proteins in amphipols, Arch. Biochem. Biophys. 564C (2014) 327–343.
[48] D.K. Debnath, D.E. Otzen, Cell-free synthesis and folding of transmembrane OmpA reveals higher order structures and premature truncations, Biophys. Chem. 152 (2010) 80–88.
[49] J.H. Kleinschmidt, L.K. Tamm, Time-resolved distance determination by tryptophan fluorescence quenching: probing intermediates in membrane protein folding, Biochemistry 38 (1999) 4996–5005.
[50] A.W. Scotto, D. Zakim, Reconstitution of membrane proteins. Spontaneous incorporation of integral membrane proteins into preformed bilayers of pure phospholipid, J. Biol. Chem. 263 (1988) 18500–18506.
[51] E. Frotscher, B. Danielczak, C. Vargas, A. Meister, G. Durand, S. Keller, A fluorinated detergent for membrane–protein applications, Angew. Chem. Int. Ed. Engl. 54 (2015) 5069–5073.
[52] E.J. Danoff, K.G. Fleming, Membrane defects accelerate outer membrane β-barrel protein folding, Biochemistry 54 (2015) 97–99.
[53] D. Marsh, B. Shanmugavadivu, J.H. Kleinschmidt, Membrane elastic fluctuations and the insertion and tilt of β-barrel proteins, Biophys. J. 91 (2006) 227–232.
[54] C.L. Pocanschi, G.J. Patel, D. Marsh, J.H. Kleinschmidt, Curvature elasticity and refolding of OmpA in large unilamellar vesicles, Biophys. J. 91 (2006) L75–L78.
[55] V. Anbazhagan, J. Qu, J.H. Kleinschmidt, D. Marsh, Incorporation of outer membrane protein OmpG in lipid membranes. Protein–lipid interactions and β-barrel orientation, Biochemistry 47 (2008) 6189–6198.
[56] M. Ramakrishnan, C.L. Pocanschi, J.H. Kleinschmidt, D. Marsh, Association of spin-labeled lipids with β-barrel proteins from the outer membrane of *Escherichia coli*, Biochemistry 43 (2004) 11630–11636.
[57] M. Ramakrishnan, J. Qu, C.L. Pocanschi, J.H. Kleinschmidt, D. Marsh, Orientation of β-barrel proteins OmpA and FhuA in lipid membranes, chain length dependence from infrared dichroism, Biochemistry 44 (2005) 3515–3523.
[58] J.F. Ellena, P. Lackowicz, H. Mongomery, D.S. Cafiso, Membrane thickness varies around the circumference of the transmembrane protein BtuB, Biophys. J. 100 (2011) 1280–1287.
[59] B.A. Lewis, D.M. Engelman, Lipid bilayer thickness varies linearly with acyl chain length in fluid phosphatidylcholine vesicles, J. Mol. Biol. 166 (1983) 211–217.
[60] T. Sinnige, M. Weingarth, M. Renault, L. Baker, J. Tommassen, M. Baldus, Solid-state NMR studies of full-length BamA in lipid bilayers suggest limited overall POTRA mobility, J. Mol. Biol. 426 (2014) 2009–2021.
[61] N. Noinaj, A.J. Kuszak, J.C. Gumbart, P. Lukacik, H. Chang, N.C. Easley, T. Lithgow, S.K. Buchanan, Structural insight into the biogenesis of β-barrel membrane proteins, Nature 501 (2013) 385–390.
[62] G. Patel, J.H. Kleinschmidt, The lipid-bilayer inserted membrane protein BamA of *Escherichia coli* facilitates insertion and folding of outer membrane protein A from its complex with Skp, Biochemistry 52 (2013) 3974–3986.
[63] J.H. Kleinschmidt, Membrane protein folding on the example of outer membrane protein A of *Escherichia coli*, Cell. Mol. Life Sci. 60 (2003) 1547–1558.
[64] L.M. McMorran, D.J. Brockwell, S.E. Radford, Mechanistic studies of the biogenesis and folding of outer membrane proteins in vitro and in vivo: what have we learned to date? Arch. Biochem. Biophys. 564 (2014) 265–280.
[65] P.V. Bulieris, S. Behrens, O. Holst, J.H. Kleinschmidt, Folding and insertion of the outer membrane protein OmpA is assisted by the chaperone Skp and by lipopolysaccharide, J. Biol. Chem. 278 (2003) 9092–9099.
[66] G.J. Patel, S. Behrens-Kneip, O. Holst, J.H. Kleinschmidt, The periplasmic chaperone Skp facilitates targeting, insertion and folding of OmpA into lipid membranes with a negative membrane surface potential, Biochemistry 48 (2009) 10235–10245.
[67] W. Rawicz, K.C. Olbrich, T. McIntosh, D. Needham, E. Evans, Effect of chain length and unsaturation on elasticity of lipid bilayers, Biophys. J. 79 (2000) 328–339.
[68] G.H. Huysmans, S.E. Radford, S.A. Baldwin, D.J. Brockwell, Malleability of the folding mechanism of the outer membrane protein PagP: parallel pathways and the effect of membrane elasticity, J. Mol. Biol. 416 (2012) 453–464.
[69] R.L. Thurmond, S.W. Dodd, M.F. Brown, Molecular areas of phospholipids as determined by ^{2}H NMR spectroscopy. Comparison of phosphatidylethanolamines and phosphatidylcholines, Biophys. J. 59 (1991) 108–113.
[70] M.F. Brown, R.L. Thurmond, S.W. Dodd, D. Otten, K. Beyer, Elastic deformation of membrane bilayers probed by deuterium NMR relaxation, J. Am. Chem. Soc. 124 (2002) 8471–8484.
[71] A. Ebie Tan, N.K. Burgess, D.S. DeAndrade, J.D. Marold, K.G. Fleming, Self-association of unfolded outer membrane proteins, Macromol. Biosci. 10 (2010) 763–767.
[72] S. Conlan, H. Bayley, Folding of a monomeric porin, OmpG, in detergent solution, Biochemistry 42 (2003) 9453–9465.
[73] J. Qu, C. Mayer, S. Behrens, O. Holst, J.H. Kleinschmidt, The trimeric periplasmic chaperone Skp of *Escherichia coli* forms 1:1 complexes with outer membrane proteins via hydrophobic and electrostatic interactions, J. Mol. Biol. 374 (2007) 91–105.
[74] H. Hong, S. Park, R.H. Jimenez, D. Rinehart, L.K. Tamm, Role of aromatic side chains in the folding and thermodynamic stability of integral membrane proteins, J. Am. Chem. Soc. 129 (2007) 8320–8327.
[75] K.M. Sanchez, J.E. Gable, D.E. Schlamadinger, J.E. Kim, Effects of tryptophan microenvironment, soluble domain, and vesicle size on the thermodynamics of membrane protein folding: lessons from the transmembrane protein OmpA, Biochemistry 47 (2008) 12844–12852.
[76] H. Hong, D. Rinehart, L.K. Tamm, Membrane depth-dependent energetic contribution of the tryptophan side chain to the stability of integral membrane proteins, Biochemistry 52 (2013) 4413–4421.
[77] W.M. Yau, W.C. Wimley, K. Gawrisch, S.H. White, The preference of tryptophan for membrane interfaces, Biochemistry 37 (1998) 14713–14718.
[78] W.C. Wimley, S.H. White, Experimentally determined hydrophobicity scale for proteins at membrane interfaces, Nat. Struct. Biol. 3 (1996) 842–848.
[79] K.M. Sanchez, T.J. Neary, J.E. Kim, Ultraviolet resonance Raman spectroscopy of folded and unfolded states of an integral membrane protein, J. Phys. Chem. B 112 (2008) 9507–9511.
[80] M.S. Fernández, P. Fromherz, Lipoid pH indicators as probes of electrical potential and polarity in micelles, J. Phys. Chem. 81 (1977) 1755–1761.
[81] M.B. Sankaram, P.J. Brophy, W. Jordi, D. Marsh, Fatty-acid pH titration and the selectivity of interaction with extrinsic proteins in dimyristoylphosphatidylglycerol dispersions. Spin label ESR studies, Biochim. Biophys. Acta 1021 (1990) 63–69.
[82] J.H. Kleinschmidt, J.E. Mahaney, D.D. Thomas, D. Marsh, Interaction of bee venom melittin with zwitterionic and negatively charged phospholipid bilayers: a spin-label electron spin resonance study, Biophys. J. 72 (1997) 767–778.
[83] D. Marsh, Handbook of Lipid Bilayers, 2. ed. CRC Press, Boca Raton u.a., 2013
[84] T.J. McIntosh, P.W. Holloway, Determination of the depth of bromine atoms in bilayers formed from bromolipid probes, Biochemistry 26 (1987) 1783–1788.
[85] M.C. Wiener, S.H. White, Transbilayer distribution of bromine in fluid bilayers containing a specifically brominated analogue of dioleoylphosphatidylcholine, Biochemistry 30 (1991) 6997–7008.
[86] A.S. Ladokhin, P.W. Holloway, Fluorescence of membrane-bound tryptophan octyl ester: a model for studying intrinsic fluorescence of protein–membrane interactions, Biophys. J. 69 (1995) 506–517.
[87] A. Chattopadhyay, E. London, Parallax method for direct measurement of membrane penetration depth utilizing fluorescence quenching by spin-labeled phospholipids, Biochemistry 26 (1987) 39–45.
[88] J.H. Kleinschmidt, P.V. Bulieris, J. Qu, M. Dogterom, T. den Blaauwen, Association of neighboring β-strands of outer membrane protein A in lipid bilayers revealed by site directed fluorescence quenching, J. Mol. Biol. 407 (2011) 316–332.
[89] G. Kang, I. Lopez-Pena, V. Oklejas, C.S. Gary, W. Cao, J.E. Kim, Förster resonance energy transfer as a probe of membrane protein folding, Biochim. Biophys. Acta 1818 (2012) 154–161.
[90] A.R. Fersht, A. Matouschek, L. Serrano, The folding of an enzyme. I. Theory of protein engineering analysis of stability and pathway of protein folding, J. Mol. Biol. 224 (1992) 771–782.
[91] D.P. Raleigh, K.W. Plaxco, The protein folding transition state: what are φ-values really telling us? Protein Pept. Lett. 12 (2005) 117–122.
[92] P.J. Bond, M.S. Sansom, Insertion and assembly of membrane proteins via simulation, J. Am. Chem. Soc. 128 (2006) 2697–2704.
[93] V. Anbazhagan, N. Vijay, J.H. Kleinschmidt, D. Marsh, Protein–lipid interactions with *Fusobacterium nucleatum* major outer membrane protein FomA: spin-label EPR and polarized infrared spectroscopy, Biochemistry 47 (2008) 8414–8423.
[94] P. Puntervoll, M. Ruud, L.J. Bruseth, H. Kleivdal, B.T. Høgh, R. Benz, H.B. Jensen, Structural characterization of the fusobacterial non-specific porin FomA suggests a 14-stranded topology, unlike the classical porins, Microbiology 148 (2002) 3395–3403.
[95] T.A. Walton, C.M. Sandoval, C.A. Fowler, A. Pardi, M.C. Sousa, The cavity-chaperone Skp protects its substrate from aggregation but allows independent folding of substrate domains, Proc. Natl. Acad. Sci. U. S. A. 106 (2009) 1772–1777.
[96] E.J. Danoff, K.G. Fleming, The soluble, periplasmic domain of OmpA folds as an independent unit and displays chaperone activity by reducing the self-association propensity of the unfolded OmpA transmembrane β-barrel, Biophys. Chem. 159 (2011) 194–204.
[97] J.H. Kleinschmidt, Assembly of integral membrane proteins from the periplasm into the outer membrane, in: M. Ehrmann (Ed.), The Periplasm, ASM Press, Washington 2007, pp. 30–66.
[98] A.H. Dewald, J.C. Hodges, L. Columbus, Physical determinants of β-barrel membrane protein folding in lipid vesicles, Biophys. J. 100 (2011) 2131–2140.
[99] J.E. Mogensen, D.E. Otzen, Interactions between folding factors and bacterial outer membrane proteins, Mol. Microbiol. 57 (2005) 326–346.
[100] J.C. Malinverni, T.J. Silhavy, Assembly of outer membrane β-barrel proteins: the BAM complex, Ecosal Plus (2011) http://dx.doi.org/10.1128/ecosalplus.4.3.8.
[101] T.F. Solov'eva, O.D. Novikova, O.Y. Portnyagina, Biogenesis of β-barrel integral proteins of bacterial outer membrane, Biochemistry (Mosc) 77 (2012) 1221–1236.
[102] C. Goemans, K. Denoncin, J.F. Collet, Folding mechanisms of periplasmic proteins, Biochim. Biophys. Acta 1843 (2014) 1517–1528.
[103] D. Missiakas, J.M. Betton, S. Raina, New components of protein folding in extracytoplasmic compartments of *Escherichia coli* SurA, FkpA and Skp/OmpH, Mol. Microbiol. 21 (1996) 871–884.
[104] J. Schwalm, T.F. Mahoney, G.R. Soltes, T.J. Silhavy, A role for Skp in LptD assembly in *Escherichia coli*, J. Bacteriol. 195 (2013) 3734–3742.
[105] R. Chen, U. Henning, A periplasmic protein (Skp) of *Escherichia coli* selectively binds a class of outer membrane proteins, Mol. Microbiol. 19 (1996) 1287–1294.
[106] B.M. Alba, C.A. Gross, Regulation of the *Escherichia coli* σ^E-dependent envelope stress response, Mol. Microbiol. 52 (2004) 613–619.
[107] M. Ehrmann, T. Clausen, Proteolysis as a regulatory mechanism, Annu. Rev. Genet. 38 (2004) 709–724.
[108] A.R. Duguay, T.J. Silhavy, Quality control in the bacterial periplasm, Biochim. Biophys. Acta 1694 (2004) 121–134.
[109] C. Dartigalongue, D. Missiakas, S. Raina, Characterization of the *Escherichia coli* σ^E-regulon, J. Biol. Chem. 276 (2001) 20866–20875.
[110] I.P. Korndörfer, M.K. Dommel, A. Skerra, Structure of the periplasmic chaperone Skp suggests functional similarity with cytosolic chaperones despite differing architecture, Nat. Struct. Mol. Biol. 11 (2004) 1015–1020.
[111] T.A. Walton, M.C. Sousa, Crystal structure of Skp, a prefoldin-like chaperone that protects soluble and membrane proteins from aggregation, Mol. Cell 15 (2004) 367–374.

[112] E. Bitto, D.B. McKay, Crystallographic structure of SurA, a molecular chaperone that facilitates folding of outer membrane porins, Structure 10 (2002) 1489–1498.
[113] X. Xu, S. Wang, Y.X. Hu, D.B. McKay, The periplasmic bacterial molecular chaperone SurA adapts its structure to bind peptides in different conformations to assert a sequence preference for aromatic residues, J. Mol. Biol. 373 (2007) 367–381.
[114] F.A. Saul, J.P. Arie, B. Vulliez-le Normand, R. Kahn, J.M. Betton, G.A. Bentley, Structural and functional studies of FkpA from *Escherichia coli*, a cis/trans peptidyl-prolyl isomerase with chaperone activity, J. Mol. Biol. 335 (2004) 595–608.
[115] E.B. Volokhina, J. Grijpstra, M. Stork, I. Schilders, J. Tommassen, M.P. Bos, Role of the periplasmic chaperones Skp, SurA and DegQ in outer membrane protein biogenesis in *Neisseria meningitidis*, J. Bacteriol. 193 (2011) 1612–1621.
[116] S.W. Lazar, R. Kolter, SurA assists the folding of *Escherichia coli* outer membrane proteins, J. Bacteriol. 178 (1996) 1770–1773.
[117] P.E. Rouvière, C.A. Gross, SurA, a periplasmic protein with peptidyl-prolyl isomerase activity, participates in the assembly of outer membrane porins, Genes Dev. 10 (1996) 3170–3182.
[118] A.E. Rizzitello, J.R. Harper, T.J. Silhavy, Genetic evidence for parallel pathways of chaperone activity in the periplasm of *Escherichia coli*, J. Bacteriol. 183 (2001) 6794–6800.
[119] J.G. Sklar, T. Wu, D. Kahne, T.J. Silhavy, Defining the roles of the periplasmic chaperones SurA, Skp, and DegP in *Escherichia coli*, Genes Dev. 21 (2007) 2473–2484.
[120] D. Vertommen, N. Ruiz, P. Leverrier, T.J. Silhavy, J.F. Collet, Characterization of the role of the *Escherichia coli* periplasmic chaperone SurA using differential proteomics, Proteomics 9 (2009) 2432–2443.
[121] S. Jarchow, C. Luck, A. Gorg, A. Skerra, Identification of potential substrate proteins for the periplasmic *Escherichia coli* chaperone Skp, Proteomics 8 (2008) 4987–4994.
[122] E. Bitto, D.B. McKay, Binding of phage-display-selected peptides to the periplasmic chaperone protein SurA mimics binding of unfolded outer membrane proteins, FEBS Lett. 568 (2004) 94–98.
[123] E. Bitto, D.B. McKay, The periplasmic molecular chaperone protein SurA binds a peptide motif that is characteristic of integral outer membrane proteins, J. Biol. Chem. 278 (2003) 49316–49322.
[124] M. Schlapschy, M.K. Dommel, K. Hadian, M. Fogarasi, I.P. Korndörfer, A. Skerra, The periplasmic *E. coli* chaperone Skp is a trimer in solution: biophysical and preliminary crystallographic characterization, Biol. Chem. 385 (2004) 137–143.
[125] J. Qu, S. Behrens-Kneip, O. Holst, J.H. Kleinschmidt, Binding regions of outer membrane protein A in complexes with the periplasmic chaperone Skp. A site-directed fluorescence study, Biochemistry 48 (2009) 4926–4936.
[126] B.M. Burmann, C. Wang, S. Hiller, Conformation and dynamics of the periplasmic membrane–protein-chaperone complexes OmpX-Skp and tOmpA-Skp, Nat. Struct. Mol. Biol. 20 (2013) 1265–1272.
[127] S. Okuda, E. Freinkman, D. Kahne, Cytoplasmic ATP hydrolysis powers transport of lipopolysaccharide across the periplasm in *E. coli*, Science 338 (2012) 1214–1217.
[128] L.M. McMorran, A.I. Bartlett, G.H. Huysmans, S.E. Radford, D.J. Brockwell, Dissecting the effects of periplasmic chaperones on the in vitro folding of the outer membrane protein PagP, J. Mol. Biol. 425 (2013) 3178–3191.
[129] S. Morein, A. Andersson, L. Rilfors, G. Lindblom, Wild-type *Escherichia coli* cells regulate the membrane lipid composition in a "window" between gel and non-lamellar structures, J. Biol. Chem. 271 (1996) 6801–6809.
[130] E.J. Lugtenberg, R. Peters, Distribution of lipids in cytoplasmic and outer membranes of *Escherichia coli* K12, Biochim. Biophys. Acta 441 (1976) 38–47.
[131] T. Wu, J. Malinverni, N. Ruiz, S. Kim, T.J. Silhavy, D. Kahne, Identification of a multicomponent complex required for outer membrane biogenesis in *Escherichia coli*, Cell 121 (2005) 235–245.
[132] N. Ruiz, B. Falcone, D. Kahne, T.J. Silhavy, Chemical conditionality: a genetic strategy to probe organelle assembly, Cell 121 (2005) 307–317.
[133] J.C. Malinverni, J. Werner, S. Kim, J.G. Sklar, D. Kahne, R. Misra, T.J. Silhavy, YfiO stabilizes the YaeT complex and is essential for outer membrane protein assembly in *Escherichia coli*, Mol. Microbiol. 61 (2006) 151–164.
[134] J. Werner, R. Misra, YaeT (Omp85) affects the assembly of lipid-dependent and lipid-independent outer membrane proteins of *Escherichia coli*, Mol. Microbiol. 57 (2005) 1450–1459.
[135] C.T. Webb, E. Heinz, T. Lithgow, Evolution of the β-barrel assembly machinery, Trends Microbiol. 20 (2012) 612–620.
[136] A.I. Höhr, S.P. Straub, B. Warscheid, T. Becker, N. Wiedemann, Assembly of β-barrel proteins in the mitochondrial outer membrane, Biochim. Biophys. Acta 1853 (2015) 74–88.
[137] J. Selkrig, D.L. Leyton, C.T. Webb, T. Lithgow, Assembly of β-barrel proteins into bacterial outer membranes, Biochim. Biophys. Acta 1843 (2014) 1542–1550.
[138] R. Voulhoux, J. Tommassen, Omp85, an evolutionarily conserved bacterial protein involved in outer-membrane-protein assembly, Res. Microbiol. 155 (2004) 129–135.
[139] D.P. Ricci, T.J. Silhavy, The Bam machine: a molecular cooper, Biochim. Biophys. Acta 1818 (2012) 1067–1084.
[140] K.H. Kim, S. Aulakh, M. Paetzel, The bacterial outer membrane β-barrel assembly machinery, Protein Sci. 21 (2012) 751–768.
[141] E.B. Volokhina, F. Beckers, J. Tommassen, M.P. Bos, The β-barrel outer membrane protein assembly complex of *Neisseria meningitidis*, J. Bacteriol. 191 (2009) 7074–7085.
[142] C.L. Hagan, T.J. Silhavy, D. Kahne, β-barrel membrane protein assembly by the Bam complex, Annu. Rev. Biochem. 80 (2011) 189–210.
[143] T.J. Knowles, A. Scott-Tucker, M. Overduin, I.R. Henderson, Membrane protein architects: the role of the BAM complex in outer membrane protein assembly, Nat. Rev. Microbiol. 7 (2009) 206–214.
[144] R. Voulhoux, M.P. Bos, J. Geurtsen, M. Mols, J. Tommassen, Role of a highly conserved bacterial protein in outer membrane protein assembly, Science 299 (2003) 262–265.
[145] W.T. Doerrler, C.R. Raetz, Loss of outer membrane proteins without inhibition of lipid export in an *Escherichia coli* YaeT mutant, J. Biol. Chem. 280 (2005) 27679–27687.
[146] J.G. Sklar, T. Wu, L.S. Gronenberg, J.C. Malinverni, D. Kahne, T.J. Silhavy, Lipoprotein SmpA is a component of the YaeT complex that assembles outer membrane proteins in *Escherichia coli*, Proc. Natl. Acad. Sci. U. S. A. 104 (2007) 6400–6405.
[147] C.L. Hagan, S. Kim, D. Kahne, Reconstitution of outer membrane protein assembly from purified components, Science 328 (2010) 890–892.
[148] P.Z. Gatzeva-Topalova, L.R. Warner, A. Pardi, M.C. Sousa, Structure and flexibility of the complete periplasmic domain of BamA: the protein insertion machine of the outer membrane, Structure 18 (2010) 1492–1501.
[149] P.Z. Gatzeva-Topalova, T.A. Walton, M.C. Sousa, Crystal structure of YaeT: conformational flexibility and substrate recognition, Structure 16 (2008) 1873–1881.
[150] S. Kim, J.C. Malinverni, P. Sliz, T.J. Silhavy, S.C. Harrison, D. Kahne, Structure and function of an essential component of the outer membrane protein assembly machine, Science 317 (2007) 961–964.
[151] T.J. Knowles, M. Jeeves, S. Bobat, F. Dancea, D. McClelland, T. Palmer, M. Overduin, I.R. Henderson, Fold and function of polypeptide transport-associated domains responsible for delivering unfolded proteins to membranes, Mol. Microbiol. 68 (2008) 1216–1227.
[152] R. Ward, M. Zoltner, L. Beer, H. El Mkami, I.R. Henderson, T. Palmer, D.G. Norman, The orientation of a tandem POTRA domain pair, of the β-barrel assembly protein BamA, determined by PELDOR spectroscopy, Structure 17 (2009) 1187–1194.
[153] D. Gessmann, Y.H. Chung, E.J. Danoff, A.M. Plummer, C.W. Sandlin, N.R. Zaccai, K.G. Fleming, Outer membrane beta-barrel protein folding is physically controlled by periplasmic lipid head groups and BamA, Proc. Natl. Acad. Sci. U. S. A. 111 (2014) 5878–5883.
[154] V. Robert, E.B. Volokhina, F. Senf, M.P. Bos, P. Van Gelder, J. Tommassen, Assembly factor Omp85 recognizes its outer membrane protein substrates by a species-specific C-terminal motif, PLoS Biol. 4 (2006) e377.
[155] L. Estrada Mallarino, E. Fan, M. Odermatt, M. Müller, M. Lin, J. Liang, M. Heinzelmann, F. Fritsche, H.J. Apell, W. Welte, TtOmp85, a β-barrel assembly protein, functions by barrel augmentation, Biochemistry 54 (2015) 844–852.
[156] C.L. Hagan, D.B. Westwood, D. Kahne, Bam lipoproteins assemble BamA in vitro, Biochemistry 52 (2013) 6108–6113.
[157] A. Arora, F. Abildgaard, J.H. Bushweller, L.K. Tamm, Structure of outer membrane protein A transmembrane domain by NMR spectroscopy, Nat. Struct. Biol. 8 (2001) 334–338.
[158] A. Pautsch, G.E. Schulz, Structure of the outer membrane protein A transmembrane domain, Nat. Struct. Biol. 5 (1998) 1013–1017.
[159] A. Pautsch, G.E. Schulz, High-resolution structure of the OmpA membrane domain, J. Mol. Biol. 298 (2000) 273–282.
[160] L. Vandeputte-Rutten, R.A. Kramer, J. Kroon, N. Dekker, M.R. Egmond, P. Gros, Crystal structure of the outer membrane protease OmpT from *Escherichia coli* suggests a novel catalytic site, EMBO J. 20 (2001) 5033–5039.
[161] C.J. Oomen, P. Van Ulsen, P. Van Gelder, M. Feijen, J. Tommassen, P. Gros, Structure of the translocator domain of a bacterial autotransporter, EMBO J. 23 (2004) 1257–1266.
[162] B. van den Berg, P.N. Black, W.M. Clemons Jr., T.A. Rapoport, Crystal structure of the long-chain fatty acid transporter FadL, Science 304 (2004) 1506–1509.
[163] R. Albrecht, M. Schutz, P. Oberhettinger, M. Faulstich, I. Bermejo, T. Rudel, K. Diederichs, K. Zeth, Structure of BamA, an essential factor in outer membrane protein biogenesis, Acta Crystallogr. D Biol. Crystallogr. 70 (2014) 1779–1789.
[164] D. Forst, W. Welte, T. Wacker, K. Diederichs, Structure of the sucrose-specific porin ScrY from *Salmonella typhimurium* and its complex with sucrose, Nat. Struct. Biol. 5 (1998) 37–46.
[165] D.P. Chimento, A.K. Mohanty, R.J. Kadner, M.C. Wiener, Crystallization and initial X-ray diffraction of BtuB, the integral membrane cobalamin transporter of *Escherichia coli*, Acta Crystallogr. D Biol. Crystallogr. 59 (2003) 509–511.
[166] G. Phan, H. Remaut, T. Wang, W.J. Allen, K.F. Pirker, A. Lebedev, N.S. Henderson, S. Geibel, E. Volkan, J. Yan, M.B. Kunze, J.S. Pinkner, B. Ford, C.W. Kay, H. Li, S.J. Hultgren, D.G. Thanassi, G. Waksman, Crystal structure of the FimD usher bound to its cognate FimC-FimH substrate, Nature 474 (2011) 49–53.
[167] S. Qiao, Q. Luo, Y. Zhao, X.C. Zhang, Y. Huang, Structural basis for lipopolysaccharide insertion in the bacterial outer membrane, Nature 511 (2014) 108–111.
[168] S. Hiller, R.G. Garces, T.J. Malia, V.Y. Orekhov, M. Colombini, G. Wagner, Solution structure of the integral human membrane protein VDAC-1 in detergent micelles, Science 321 (2008) 1206–1210.
[169] M. Bayrhuber, T. Meins, M. Habeck, S. Becker, K. Giller, S. Villinger, C. Vonrhein, C. Griesinger, M. Zweckstetter, K. Zeth, Structure of the human voltage-dependent anion channel, Proc. Natl. Acad. Sci. U. S. A. 105 (2008) 15370–15375.
[170] J.S. Park, W.C. Lee, K.J. Yeo, K.S. Ryu, M. Kumarasiri, D. Hesek, M. Lee, S. Mobashery, J.H. Song, S.I. Kim, J.C. Lee, C. Cheong, Y.H. Jeon, H.Y. Kim, Mechanism of anchoring of OmpA protein to the cell wall peptidoglycan of the Gram-negative bacterial outer membrane, FASEB J. 26 (2012) 219–228.
[171] W.L. Delano, The PyMOL Molecular Graphics System, DeLano Scientific, San Carlos, CA, U.S.A., 2002
[172] S. Okuda, H. Tokuda, Lipoprotein sorting in bacteria, Annu. Rev. Microbiol. 65 (2011) 239–259.
[173] N. Ruiz, D. Kahne, T.J. Silhavy, Advances in understanding bacterial outer-membrane biogenesis, Nat. Rev. Microbiol. 4 (2006) 57–66.
[174] A.D. Ferguson, W. Welte, E. Hofmann, B. Lindner, O. Holst, J.W. Coulton, K. Diederichs, A conserved structural motif for lipopolysaccharide recognition by procaryotic and eucaryotic proteins, Structure 8 (2000) 585–592.

[175] S. Behrens, R. Maier, H. de Cock, F.X. Schmid, C.A. Gross, The SurA periplasmic PPIase lacking its parvulin domains functions in vivo and has chaperone activity, EMBO J. 20 (2001) 285–294.
[176] H. Hong, D.R. Patel, L.K. Tamm, B. van den Berg, The outer membrane protein OmpW forms an eight-stranded β-barrel with a hydrophobic channel, J. Biol. Chem. 281 (2006) 7568–7577.
[177] J. Vogt, G.E. Schulz, The structure of the outer membrane protein OmpX from *Escherichia coli* reveals possible mechanisms of virulence, Struct. Fold. Des. 7 (1999) 1301–1309.
[178] C. Fernandez, C. Hilty, G. Wider, P. Guntert, K. Wüthrich, NMR structure of the integral membrane protein OmpX, J. Mol. Biol. 336 (2004) 1211–1221.
[179] L. Vandeputte-Rutten, M.P. Bos, J. Tommassen, P. Gros, Crystal structure of *neisserial* surface protein A (NspA), a conserved outer membrane protein with vaccine potential, J. Biol. Chem. 278 (2003) 24825–24830.
[180] V.E. Ahn, E.I. Lo, C.K. Engel, L. Chen, P.M. Hwang, L.E. Kay, R.E. Bishop, G.G. Prive, A hydrocarbon ruler measures palmitate in the enzymatic acylation of endotoxin, EMBO J. 23 (2004) 2931–2941.
[181] P.M. Hwang, W.Y. Choy, E.I. Lo, L. Chen, J.D. Forman-Kay, C.R. Raetz, G.G. Prive, R.E. Bishop, L.E. Kay, Solution structure and dynamics of the outer membrane enzyme PagP by NMR, Proc. Natl. Acad. Sci. U. S. A. 99 (2002) 13560–13565.
[182] S.M. Prince, M. Achtman, J.P. Derrick, Crystal structure of the OpcA integral membrane adhesin from *Neisseria meningitidis*, Proc. Natl. Acad. Sci. U. S. A. 99 (2002) 3417–3421.
[183] J. Ye, B. van den Berg, Crystal structure of the bacterial nucleoside transporter Tsx, EMBO J. 23 (2004) 3187–3195.
[184] H.J. Snijder, I. Ubarretxena-Belandia, M. Blaauw, K.H. Kalk, H.M. Verheij, M.R. Egmond, N. Dekker, B.W. Dijkstra, Structural evidence for dimerization-regulated activation of an integral membrane phospholipase, Nature 401 (1999) 717–721.
[185] O. Yildiz, K.R. Vinothkumar, P. Goswami, W. Kühlbrandt, Structure of the monomeric outer-membrane porin OmpG in the open and closed conformation, EMBO J. 25 (2006) 3702–3713.
[186] G.V. Subbarao, B. van den Berg, Crystal structure of the monomeric porin OmpG, J. Mol. Biol. 360 (2006) 750–759.
[187] D. Ni, Y. Wang, X. Yang, H. Zhou, X. Hou, B. Cao, Z. Lu, X. Zhao, K. Yang, Y. Huang, Structural and functional analysis of the β-barrel domain of BamA from *Escherichia coli*, FASEB J. 28 (2014) 2677–2685.
[188] K. Zeth, K. Diederichs, W. Welte, H. Engelhardt, Crystal structure of Omp32, the anion-selective porin from *Comamonas acidovorans*, in complex with a periplasmic peptide at 2.1 Å resolution, Struct. Fold. Des. 8 (2000) 981–992.
[189] M.S. Weiss, A. Kreusch, E. Schiltz, U. Nestel, W. Welte, J. Weckesser, G.E. Schulz, The structure of porin from *Rhodobacter capsulatus* at 1.8 Å resolution, FEBS Lett. 280 (1991) 379–382.
[190] M.S. Weiss, G.E. Schulz, Structure of porin refined at 1.8 Å resolution, J. Mol. Biol. 227 (1992) 493–509.
[191] A. Kreusch, G.E. Schulz, Refined structure of the porin from *Rhodopseudomonas blastica*. Comparison with the porin from *Rhodobacter capsulatus*, J. Mol. Biol. 243 (1994) 891–905.
[192] S.W. Cowan, T. Schirmer, G. Rummel, M. Steiert, R. Ghosh, R.A. Pauptit, J.N. Jansonius, J.P. Rosenbusch, Crystal structures explain functional properties of two *E. coli* porins, Nature 358 (1992) 727–733.
[193] R. Dutzler, G. Rummel, S. Alberti, S. Hernandez-Alles, P. Phale, J. Rosenbusch, V. Benedi, T. Schirmer, Crystal structure and functional characterization of OmpK36, the osmoporin of *Klebsiella pneumoniae*, Struct. Fold. Des. 7 (1999) 425–434.
[194] T. Schirmer, T.A. Keller, Y.F. Wang, J.P. Rosenbusch, Structural basis for sugar translocation through maltoporin channels at 3.1 Å resolution, Science 267 (1995) 512–514.
[195] Y.F. Wang, R. Dutzler, P.J. Rizkallah, J.P. Rosenbusch, T. Schirmer, Channel specificity: structural basis for sugar discrimination and differential flux rates in maltoporin, J. Mol. Biol. 272 (1997) 56–63.
[196] J.E. Meyer, M. Hofnung, G.E. Schulz, Structure of maltoporin from *Salmonella typhimurium* ligated with a nitrophenyl-maltotrioside, J. Mol. Biol. 266 (1997) 761–775.
[197] A.D. Ferguson, E. Hofmann, J.W. Coulton, K. Diederichs, W. Welte, Siderophore-mediated iron transport: crystal structure of FhuA with bound lipopolysaccharide, Science 282 (1998) 2215–2220.
[198] K.P. Locher, B. Rees, R. Koebnik, A. Mitschler, L. Moulinier, J.P. Rosenbusch, D. Moras, Transmembrane signaling across the ligand-gated FhuA receptor: crystal structures of free and ferrichrome-bound states reveal allosteric changes, Cell 95 (1998) 771–778.
[199] S.K. Buchanan, B.S. Smith, L. Venkatramani, D. Xia, L. Esser, M. Palnitkar, R. Chakraborty, D. van der Helm, J. Deisenhofer, Crystal structure of the outer membrane active transporter FepA from *Escherichia coli*, Nat. Struct. Biol. 6 (1999) 56–63.
[200] A.D. Ferguson, R. Chakraborty, B.S. Smith, L. Esser, D. van der Helm, J. Deisenhofer, Structural basis of gating by the outer membrane transporter FecA, Science 295 (2002) 1715–1719.
[201] W.W. Yue, S. Grizot, S.K. Buchanan, Structural evidence for iron-free citrate and ferric citrate binding to the TonB-dependent outer membrane transporter FecA, J. Mol. Biol. 332 (2003) 353–368.
[202] D.P. Chimento, A.K. Mohanty, R.J. Kadner, M.C. Wiener, Substrate-induced transmembrane signaling in the cobalamin transporter BtuB, Nat. Struct. Biol. 10 (2003) 394–401.
[203] G. Kurisu, S.D. Zakharov, M.V. Zhalnina, S. Bano, V.Y. Eroukova, T.I. Rokitskaya, Y.N. Antonenko, M.C. Wiener, W.A. Cramer, The structure of BtuB with bound colicin E3 R-domain implies a translocon, Nat. Struct. Biol. 10 (2003) 948–954.
[204] D. Cobessi, H. Celia, N. Folschweiller, I.J. Schalk, M.A. Abdallah, F. Pattus, The crystal structure of the pyoverdine outer membrane receptor FpvA from *Pseudomonas aeruginosa* at 3.6 Å resolution, J. Mol. Biol. 347 (2005) 121–134.
[205] H. Remaut, C. Tang, N.S. Henderson, J.S. Pinkner, T. Wang, S.J. Hultgren, D.G. Thanassi, G. Waksman, H. Li, Fiber formation across the bacterial outer membrane by the chaperone/usher pathway, Cell 133 (2008) 640–652.
[206] V. Koronakis, A. Sharff, E. Koronakis, B. Luisi, C. Hughes, Crystal structure of the bacterial membrane protein TolC central to multidrug efflux and protein export, Nature 405 (2000) 914–919.
[207] M. Faller, M. Niederweis, G.E. Schulz, The structure of a mycobacterial outer-membrane channel, Science 303 (2004) 1189–1192.
[208] L. Song, M.R. Hobaugh, C. Shustak, S. Cheley, H. Bayley, J.E. Gouaux, Structure of staphylococcal α-hemolysin, a heptameric transmembrane pore, Science 274 (1996) 1859–1866.